

Characterising the Cell Surface proteins in ARID1A-deficient Gastric Cancer

A Thesis

submitted to

Indian Institute of Science Education and Research Pune in partial fulfilment of the
requirements for the BS-MS Dual Degree Programme

by

Aditi Singh



Indian Institute of Science Education and Research Pune
Dr. Homi Bhabha Road,
Pashan, Pune 411008, INDIA.

Date: 17th March, 2024

Under the guidance of
Dr. Anand D. Jeyasekharan
Cancer Science Institute, National University of Singapore
From August 7th 2023 to April 9th 2024

INDIAN INSTITUTE OF SCIENCE EDUCATION AND RESEARCH PUNE

Certificate

This is to certify that this dissertation entitled **Characterising the Cell Surface proteins in ARID1A-deficient Gastric Cancer** towards the partial fulfilment of the BS-MS dual degree programme at the Indian Institute of Science Education and Research, Pune represents study/work carried out by Aditi Singh at the Cancer Science Institute, National University of Singapore under the supervision of **Dr. Anand D. Jeyasekharan** – Assistant Professor, Department of Medicine, National University of Singapore, during the academic year 2023-2024.



Dr. Anand D. Jeyasekharan

Committee:

Dr. Anand D. Jeyasekharan

Dr. Kundan Sengupta

This thesis is dedicated to a future without cancer

Declaration

I hereby declare that the matter embodied in the report entitled **Characterising the Cell Surface proteins in ARID1A-deficient Gastric Cancer** are the results of the work carried out by me at the Cancer Science Institute, National University of Singapore, under the supervision of Dr. Anand D. Jeyasekharan and the same has not been submitted elsewhere for any other degree. Wherever others contribute, every effort is made to indicate this clearly, with due reference to literature and acknowledgement of collaborative research and discussions.



Aditi Singh
20191216
IISER-Pune

29th April 2024

Acknowledgements

I would like to express my gratitude to Dr. Anand D. Jeyasekharan for providing me with the opportunity to complete my master's project in his lab and for his commitment in fostering a supportive and encouraging learning environment. I would also like to mention my TAC members Dr. Kundan Sengupta and Dr. Krishanpal Karmodiya for their valuable feedback. A special token of thanks to Dr. Patrick Jaynes William who made sure everything was on track and helped in procuring everything necessary.

I would like to appreciate the constant guidance of Norbert Tay, my PhD mentor throughout the course of my project. A special thanks to Shruti, Akshaya and Rui Xue as well as other members of the lab who have always been there to help me in times of need. I would also like to thank CSI, NUS and IISER-Pune Biology department to provide me this opportunity and KVPY for their financial support. I would like to acknowledge Pundrik Sumedha and Wai Khang (Dr. Dennis Kappei Lab) whose contribution and help have been indispensable to this project.

I am extremely grateful to Vachan SJ who has been there for me through my highs and lows, and without whom Singapore wouldn't have felt like home. I should also thank my friends Chaitanya and Archana for helping settle around in a new place.

Lastly, I would like to thank Asmita, Ishan, and my mom for always for cheering and supporting me even though they are miles away.

Abstract

Chromatin remodellers play a pivotal role in controlling gene expression thereby playing prominent roles in tumour progression. AT-Rich Interacting Domain 1A (ARID1A) is a non-catalytic subunit of the SWI/SNF chromatin remodelling complex that is frequently mutated in various cancers. Gastric cancer is one of the leading causes of cancer mortality across the world and harbours *ARID1A* mutation in about 30% of cases. Despite being implicated with various synthetic lethal targets, there remains to be limited clinical efficacy associated with ARID1A deficiency in tumour cells.

The cellular surface proteome, often referred to as the 'surfaceome,' acts as a vital interface between afflicted cells and their immediate microenvironment. Within the context of cancer, this domain not only defines the biology of tumours but also represents a valuable reservoir of potential biomarkers targets for therapy. Here, we try to characterize the surfaceome in non-isogenic ARID1A-deficient and ARID1A Wild-Type (WT) gastric cancer cell lines to compare and identify specific protein targets that can negatively influence the tumour microenvironment (TME) or act as potential drug targets. This was followed by an *in-silico* transcriptome analysis from TCGA to validate our findings as well as to gain probable mechanistic insights into the function of ARID1A-deficient tumour cells.

Interestingly, we report the enrichment of proteins that primarily regulate migration, metastasis and proteins that lead to an immunosuppressive TME. In concert with these findings, we also found a significant enrichment of mitochondrial genes that regulate oxidative phosphorylation which several other studies have found in SWI/SNF-deficient tumours.

Contributions

Contributor name	Contributor role
Dr. Anand D. Jeyasekharan	Conceptualization Ideas
Wai Khang, Norbert Tay	Methodology
Vartika Kanchandani, Pundrik Sumedha, Hong Liang, Shruti Shridhar	Formal analysis
Cancer Science Institute, Singapore Dr. Anand D. Jeyasekharan	Resources
Norbert Tay, Patrick Jaynes William	Writing - review and editing
MMA Core, CSI	Visualization
Norbert Tay	Supervision
Dr. Anand D. Jeyasekharan	Funding acquisition

Contents

Abstract	xi
1 Background & Introduction	9
1.1 Aims & Objective	12
2 Methods	14
2.1 Cell-Line & Cell cultures	14
2.2 Flow-cytometry	14
2.3 Immunofluorescence Assay	14
2.4 Cell-Surface Protein Isolation using biotin-streptavidin	15
2.5 Western Blotting	15
2.6 Mass Spectrometry	15
2.7 ARID1A Overexpression cell lines	15
2.8 RNA-Sequencing	16
3 Results	17
3.1 Cell-surface proteins can be efficiently enriched using Biotin-Streptavidin interaction	17
3.2 ARID1A-deficient cell lines specifically enriched for cell-surface proteins involved in immunosuppression and cell migration	23
3.3 RNA-seq analysis further validated the role of immunosuppressive modulators in ARID1A-deficient Gastric Cancer patients	26
3.4 ARID1A and mitochondrial metabolism	28
4 Discussion	29
References	31
Supplementary Figures	38

List of Figures

Figure 1. Current therapy options for ARID1A-deficient cancers. Cited by Mandal et al. (2022)	10
Figure 2. Cell viability curve for 3 ARID1A-wildtype(red) & 3 ARID1A-mutant(blue) GC cell lines using several different drugs known to have synthetic lethal effects on ARID1A-mutant cells.....	12
Figure 3. Structure of sulfo-NHS-SS-biotin molecule and it's mechanism of action.....	17
Figure 4. Overall methodology of cell-surface protein isolation and identification.....	18
Figure 5. Flow-cytometry - Fluorescence peaks indicating biotinylated (red), non-biotinylated control (yellow) and unstained samples (blue). Figures a & b represent the following peaks at 0.5 mg/mL concentration of biotin solution in AGS and NUGC-4 cell	18
Figure 6. Fluorescence images AGS and NUGC-3 at 0.5 mg/mL biotin solution. (N=1, n=3)	19
Figure 7. ARID1A & EGFR expression in ten different gastric cancer cell lines - ARID1A WT (AGS, HGC-27, SNU-16, KATO III, NUGC-4) and ARID1A mutants (SNU-1, SNU-5, NUGC-3, OCUM-1, IM95). Western blot analysis showed absence of ARID1A expression in SNU-1,	20
Figure 8. Biotin-streptavidin pull-down validation - Western blot confirming effective binding and isolation of the cell-surface proteins. The proteins were run on a 10% acrylamide gel for SDS-PAGE. (N=4 for each cell line).....	21
Figure 9. Bar plots for GO term analysis in AGS, NUGC-4, OCUM-1, SNU-1, SNU-5 cells -. Each cell-type has 3 plots comparing enrichment of proteins between biotinylated (pull-down) vs non-biotinylated (control), biotinylated vs input and input vs biotinyl	22-23
Figure 10. Venn diagrams show the number of unique and common proteins that were enriched in the biotinylated groups compared to the non-biotinylated controls in ARID1A-mutant & ARID1A-wt cell lines. The common surface proteins in the ARID1A-wt (219) an.....	24
Figure 11. ARID1A gene expression plot – Figure shows ARID1A expression in 412 patients in the TCGA cohort with a median gene expression value of ~12 units. The ARID1A low and high cut-offs were made based on this expression pattern of ARID1A.....	27
Figure 12. Volcano plot showing DEGs in ARID1A-high vs low tumours – Cut-off values for enriched proteins is value $>\log_2fc(0.5)$ and p-value <0.05	27
Figure 13. Enriched pathways in the DEGs between ARID1A-high vs low tumours.....	28
Figure 14. IDO-1, MIF and ANXA-1 can be possibly targeted using drugs to control immunosuppression and metastasis.	30

Chapter 1

Introduction

Chromatin remodelling complexes make it possible for cells to acquire extremely diverse functional and morphological states in the body, despite sharing the same DNA by regulating chromatin accessibility and thereby influencing gene expression. The growing literature on these complexes in humans highlights the importance that they play in pathological conditions like cancer [1,2,3]. Amongst these, mutations in the genes encoding the subunits of SWI/SNF (Switch/Sucrose non-fermentable) chromatin remodelling complex are the most frequent, collectively occurring in about 25% of all cancers [4,5,6]. The mammalian SWI/SNF complexes, also known as BRG1/BRM associated factor (BAF) complex belong to three broad subfamilies – canonical BAF (cBAF); polybromo BAF (PBAF); and the GLTSCR1 or GLTSCR1L-containing and BRD9-containing non-canonical BAF (ncBAF). All three complexes contain the core catalytic subunits including SMARCC1, SMARCC2, and either of the ATPases SMARCA4 or SMARCA2, but also contain numerous non-catalytic subunits that provide each of the complexes with a distinct identity [6].

Amongst the genes encoding the subunits of the SWI/SNF complex, *AT-rich interactive domain 1A* or *ARID1A* is the most frequently mutated gene across all cancers with about 50% of ovarian clear cell carcinoma (OCCCs) and about 25%-30% of all gastric cancers (GCs)[7,8,9,10,11,12]. *ARID1A* is located on chromosome 1p36.11 and encodes a large protein with a molecular weight of about 250kD. It is a core non-catalytic subunit of the ATP-dependent cBAF complex. The ARID1A protein comprises two conserved regions: the N-terminal ARID (AT-rich interactive domain) domain and the C-terminal section containing three LXXLL motifs [13]. While the ARID domain is believed to be pivotal in enhancing BAF's chromatin affinity for specific targets in vivo, the C-terminal domain facilitates interactions between various proteins and nuclear hormone receptors [14]. Both ARID1A and its counterpart ARID1B share an ARID DNA-binding domain along with a homologous domain of uncertain function. Although the precise role of this carboxy-terminal domain remains unclear, it is speculated to possess ubiquitin ligase activity. [15].

Multiple studies provide cogent evidence highlighting the functional role of ARID1A as a tumour suppressor [16,17,18,19]. Aberrations in chromatin remodelers often increase oncogene addiction in these tumour cells making them potential synthetic lethal drug targets [20]. Synthetic lethality is a phenomenon where the simultaneous loss of function of two genes causes cell death, whereas the inactivation of any one of two genes independently has no impact on cell survival. Studies indicate a gene-dose dependent role for ARID1A in tumour suppression [7] and likely follows the classical Knudson 'two-hit' model of tumour suppression [21,22]. Currently, there are several preclinical studies and ongoing clinical trials to identify viable and efficient synthetic lethal therapeutic targets for ARID1A-mutant cases [23].

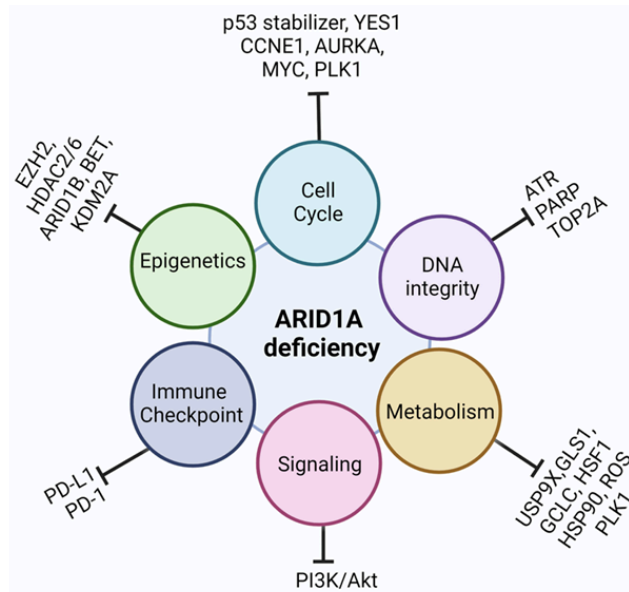


Figure 1. Current therapy options for ARID1A-deficient cancers. Figure reproduced from ref. [85] in accordance with the Creative Commons license, CC by 4.0 (<https://creativecommons.org/licenses/by/4.0/>) Mandal et al. (2022)

The PI3K/Akt/mTOR pathway is an important growth and survival pathway in healthy cells, which is often abused by malignant cells to proliferate unchecked in the pretext of cancer [24]. Aberrations in the PI3K/Akt/mTOR pathway are one of the most common genomic abnormalities in a variety of cancers. Several studies report that *ARID1A* mutations frequently co-occur with mutations that lead to the activation of PIK3/Akt signalling pathways such as loss of *PTEN* and gain-of-function mutations of the *PIK3CA* gene which encodes the catalytic subunit of the p110 α of PIK3 [25,26]. Chandler et. al also showed that *ARID1A-PIK3CA* mutations co-occurring in ovarian clear cell carcinoma (OCCC) induces inflammation-driven tumorigenesis via sustained IL-6 production. IL-6 is an inflammatory cytokine that triggers JAK/STAT3 signalling and has prominent roles in tumor cell growth and differentiation [21]. Elevated levels of circulating IL-6 in patients with OCCC are linked to unfavorable prognoses, suggesting that targeting IL-6 with an anti-IL-6 antibody like Siltuximab could offer a safe therapeutic approach for these patients. [21].

One of the possible underlying mechanisms of regulation of the PI3K/Akt signalling maybe through the PI3K-interacting protein 1 (PIK3IP1), an inhibitor of the PI3K/Akt pathway. ARID1A binds to the promoter of *PIK3IP1* driving its expression [27]. However, in ARID1A-deficient cancer cells, PIK3IP1 expression is decreased leading to the activation of the PI3K/Akt/mTOR pathway [28]. In addition to this, Polycomb Repressive Complex 2 (PRC2) has long been known to have functional antagonism to the SWI/SNF complex [29,30]. The extensively studied catalytic subunit of the PRC2 complex, Enhancer of Zeste 2 (EZH2) functions as a methyltransferase and mediates gene repression and promotes oncogenesis in a variety of cancers [31]. It is speculated to interact and repress *PIK3IP1* gene, however in the presence of ARID1A this function is dominated by the activating signals of the SWI/SNF complex. In the absence of ARID1A, EZH2 represses the expression of the PIK3IP1 and promotes the PI3K/Akt/mTOR pathway [28]. Furthermore, Li. et al reported that ARID1A interacts with EZH2 by its C-terminal domain and antagonises its IFN responsiveness and immune evasion via reduced IFN gene chromatin accessibility [32]. This led to poor immunogenicity of OCCC tumours, which contradicts the majority of other reports that

correlate ARID1A deficiency to positive effects on tumour immunity and patient response to immune checkpoint blockade (ICB) therapies like anti-PD-L1 antibodies [33]. Another study showed that HDAC2 acts as a co-repressor of EZH2 in the absence of ARID1A to suppress the expression of genes like PIK3IP1 to inhibit apoptosis and promote proliferation [28].

Double-stranded breaks (DSBs) in the DNA during replication stress are usually repaired by the error-proof homologous recombination repair (HRR)[20]. The inability to sustain an efficient DSB repair makes the cells opt for an alternate highly-error prone non-homologous end-joining (NHEJ) repair pathway [34]. Studies have shown that overactivation of the PI3K/Akt pathway suppresses the HRR of DNA DSBs by several mechanisms like suppressing HRR by the action of p70S6 kinase-dependent downregulation of MRE11[35]. Another mechanism by which the PI3K/AKT pathway inhibits the HRR is by hindering the nuclear localisation of Rad51 and BRCA1 proteins [36,37]. Due to *ARID1A* gene's established correlation with the PI3K pathway, a recent study by VA Yakovlev and colleagues demonstrated that ARID1A deficiency led to attenuation of HRR by stimulating the PI3K/AKT pathway making the cells sensitive to PARP inhibitors [38]. Additionally, a critical role of ARID1A in regulating the DNA damage checkpoint involves its recruitment to DNA double-strand breaks (DSBs) through interaction with the upstream DNA damage checkpoint kinase ATR [39]. At a molecular level, ARID1A facilitates the efficient processing of DSBs into single-strand ends. Consequently, the absence of ARID1A renders cancer cells more susceptible to PARP inhibitors both in vitro and in vivo models [40]. However, the effectiveness of PARP inhibitors in patients with ARID1A alterations remains uncertain. Hu et al. conducted screenings on several breast and ovarian cancer cell lines and found that loss of ARID1A conferred resistance to PARP inhibition therapy [41].

In gastric cancer, ARID1A mutations are usually associated with Epstein-Barr virus (EBV) positive and microsatellite instability (MSI) subtype/ DNA mismatch repair (MMR) protein deficiency and are characterised by frequent overexpression of PD-L1/L2, CDKN2A methylation, PIK3CA mutations and relatively less TP53 mutations [42,43]. ARID1A has been implicated with MMR-deficiency as it works to recruit MSH2 during replication and inactivation of ARID1A leads to functional impairment of MMR and accumulation of gene mutations [33,28]. Due to its established roles in DNA damage repair mechanisms, it has been hypothesised that ARID1A-deficiency causing alterations in the DNA damage pathways leads to increased genomic instability & mutagenesis in the cell leading to the production of increased neoantigens on the cell surface [44,33]. An analysis of 14 gastric cancer cohorts showed that ARID1A-deficient GCs showed increased expression of PD-L1 and correlated with decreased overall survival in patients. These studies indicate that immune checkpoint inhibition therapies like anti-PDL1 therapies may be a good therapeutic option of ARID1A deficient patients in GC [45].

A recent study by S. Wu validated the use of a glutaminase inhibitor to suppress the growth of ARID1A mutants, but not wildtype, OCCCs in both orthotopic and patient-derived xenografts. The SWI/SNF complex represses glutaminase (GLS1) and they reported that ARID1A inactivation led to the upregulation of GLS1[46]. GLS1 is a mitochondrial enzyme that hydrolyses glutamine into glutamate and fuels rapid proliferation, invasion and metastatic colonization of cancer cells [47]. In addition, glutaminase inhibition was shown to work in synergy with ICB anti-PDL1 antibody in a genetic OCCC mouse model driven by conditional ARID1A inactivation[46]. Newer targets that affect tumour metabolism are now being extensively studied as potential combination therapy options. A previous study by our lab revealed that ARID1A-deficient cells display an unusual mitochondrial phenotype making them more vulnerable to Polo-like kinase 1 (PLK1) inhibition[47]. Lastly, ARID1A mutated cancer cells have been found to be sensitive to ROS-inducing agents like elescomol compared to ARID1A-WT cells[48]. Ogiwara et al. established a

connection between ARID1A and glutathione metabolism, which is mediated through the regulation of the cystine/glutamate transporter XCT. This discovery underscores that reduced glutathione synthesis represents a metabolic vulnerability in cancers harbouring ARID1A-inactivating mutations. [49].

In contexts unrelated to cancer, research has brought attention to germline mutations in SWI/SNF genes as contributors to various intellectual disability syndromes. Specifically, ARID1B haploinsufficiency has emerged as a likely factor in causing abnormalities in the corpus callosum and concurrent intellectual disabilities among several patients. Subsequently, Hoyer et al. [61] reported ARID1B haploinsufficiency in 0.9% of an unselected group of 887 patients with unexplained intellectual disability. Alterations in SWI/SNF genes such as ARID1B, ARID1A, SMARCA4, SMARCE1, and SMARCB1 have been associated with Coffin-Siris Syndrome, a rare intellectual disability disorder characterized by various manifestations including hypoplasia of the distal phalanx or nail of the fifth and additional digits, hypotonia, and distinctive facial features [62].

1.1 Aims and Objectives

The majority of the currently studied therapies for ARID1A-deficient cancers are conducted in cell lines and isogenic mouse models and show promising results only in these pre-clinical settings. None of these studies have been able to translate into very successful clinical trials. Moreover, most of the studies show pre-clinical relevance and significance only in gynaecological cancers. Studies from our lab using an extensive drug panel (Supplementary Fig. 1) targetting various synthetic lethal targets in non-isogenic GC cell lines did not show any significant difference in cell viability between ARID1A-wildtype and mutant cell lines.

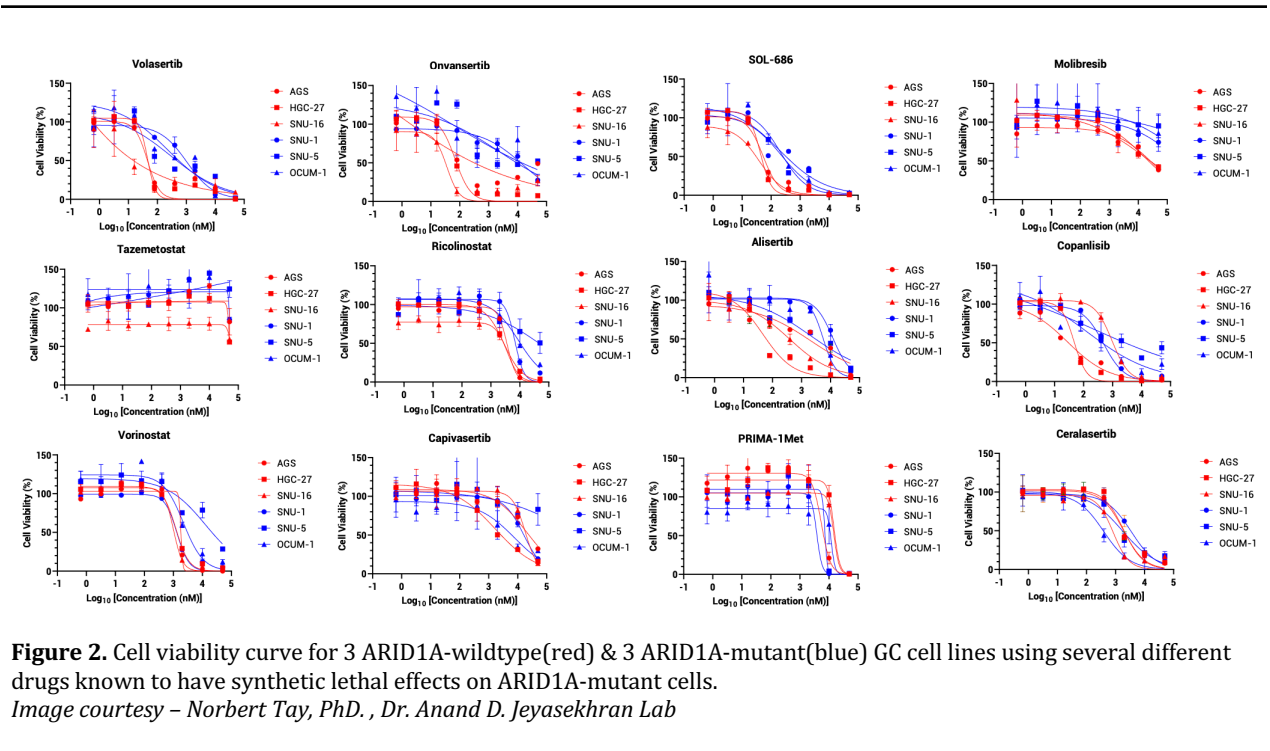


Figure 2. Cell viability curve for 3 ARID1A-wildtype(red) & 3 ARID1A-mutant(blue) GC cell lines using several different drugs known to have synthetic lethal effects on ARID1A-mutant cells.

Image courtesy – Norbert Tay, PhD., Dr. Anand D. Jeyasekhran Lab

This may be because of the inherent variability between different cancers as well as the heterogeneous nature of tumours. Moreover, the biological implications from one model system may not essentially translate to another system. This indicates that the functional roles of ARID1A are context-dependent and has broader implications on cell functioning than anticipated.

The tumour microenvironment (TME) plays a significant role in regulating tumour growth, with cell-surface proteins serving as crucial mediators of communication between the TME and tumour cells. Given that ARID1A's primary function involves transcription regulation, we propose that it could also impact the expression of specific membrane proteins, thereby affecting cancer cell survival and proliferation. Consequently, identifying differentially expressed cell-surface proteins in ARID1A-deficient cells could pinpoint potential therapeutic targets for intervention.

Therefore, the main objective of this project was to isolate, identify and compare the cell-surface protein repertoire between ARID1A WT vs mutant/deficient GC cell lines and look for differentially expressed surface proteins that can be promising drug targets for cancer therapy in ARID1A-deficient tumours. To this end, we use a biotin-streptavidin system to co-immunoprecipitate cell-surface proteins and analyse the proteins through mass spectrometry. In addition to this, we also did an RNA-sequencing analysis using the TCGA-STAD (stomach adenocarcinoma) datasets for a more comprehensive understanding of the pathogenesis associated with ARID1A in gastric cancer.

Chapter 2

Methods

2.1 Cell-Lines and cell cultures

Cell lines were grown and cultured in RPMI or DMEM medium in 100 mm culture dishes in standard conditions at 37°C in 5% CO₂. The media was supplemented with 10% fetal bovine serum (FBS) and other cell-lines specific additives. Cells were split regularly after reaching 80%-85% confluency. The following table enlists different cell lines with their required media components.

Cell Line	Media Components
AGS	RPMI-1640 + 10%FBS + 1%NEAA
NUGC-4	RPMI-1640 + 10%FBS + 1%NEAA
SNU-1	RPMI-1640 + 10%FBS + 1%NEAA
SNU-5	RPMI-1640 + 10%FBS + 1%NEAA
NUGC-3	RPMI-1640 + 10%FBS + 1%NEAA
OCUM-1	DMEM + 10%FBS + 1%NEAA + 0.5mM Sodium Pyruvate
HEK293T	DMEM + 10%FBS

2.2 Flow-cytometry

For efficient extraction, the first step is to decide an optimal concentration of biotin solution to efficiently tag surface membrane proteins. For this, 1 million cells were seeded in culture plates 48h before biotinylation. For biotinylation, the cells were incubated with different concentration of cold biotin solution in PBS on ice or in 4°C for 30 mins followed by quenching with 50mM glycine solution. The cells were washed in PBS, scrapped and collected followed by resuspension in FACS buffer. Finally, the samples were incubated with streptavidin-fluorophore. before analysing by Celesta FACS Analyser.

2.3 Immunofluorescence Assay

0.1 million cells were seeded in 24-well plates on a cover-slip for immunofluorescence assay (IFA). Two days prior to seeding the cells were incubated in different concentrations of cold biotin solution followed by fixing cells in 4% PFA after quenching the excess biotin in 50mM glycine in PBS. The cells were then blocked in bovine serum albumin (BSA) for one hour followed by washing with PBS thrice. The cells were then incubated with, streptavidin fluorophore & Hoescht 33342 for 1 hr followed by mounting and imaging using fluorescence microscopy.

2.4 Cell-Surface Protein Isolation using biotin-streptavidin

Cells were cultured in 15cm dishes or T75 flasks until 90%-95% confluency for adherent and suspension cells respectively. The cells were then treated with 5 mL of 0.5 mg/mL biotin (Cat No. 21331, EZ-Link™ Sulfo-NHS-SS-Biotin) solution or PBS for 30 mins on ice for treatment and control respectively followed by quenching with 10 mL of 50mM glycine solution for 15 mins on ice. After biotin treatment, the cells are collected and lysed using RIPA buffer. A part of this lysate is kept as the 'input' fraction. This input fraction contains all the cell proteins including the biotinylated as well as the non-biotinylated proteins. Further, 200uL of 3ug (total 600ug) of this lysate was incubated with streptavidin beads (magnetic beads) for 4 hours at 4°C. Post incubation, a small fraction of the supernatant was kept as the 'intracellular' or the 'flow-through' which should contain all the non-biotinylated proteins. The beads were then taken and heated to 95°C in Laemmli buffer to separate the biotin and streptavidin from the beads by denaturing it. This fraction is called the 'cell-surface' fraction containing the biotinylated proteins. These samples were then submitted for MS after validation with western blot.

2.5 Western Blotting

Protein lysates were subjected to SDS/PAGE (10% agarose gel for biotinylated pull-down samples and 7% gel for ARID1A expression gels run at 80V for 15 mins immediately followed by 110V for 60 mins) and transferred to nitrocellulose membrane overnight at 30V for 900 minutes. They were then incubated in the corresponding primary and secondary antibodies.

2.6 Mass Spectrometry

We used label-free quantification (LFQ) for analysing cell surfaceome enrichment in 5 different GC cell lines – AGS, NUGC-4 (ARID1A-WT) and SNU-1, SNU-5 and OCUM-1 (ARID1A mutants). For quantification, protein groups with LFQ intensities (non-zero values) in less than three replicates (total 4 biological replicates for each cell line) in either the treatment or control sets in all the cell lines were removed keeping rest of the MS data intact. To avoid creating unrealistic ratios, the zero values were imputed from a random distribution from the lower end of the spectrum. The variations during multiple rounds of imputation were represented as standard deviation in the final processing. For further processing, we selected proteins associated with the GO term GO0005886 (plasma membrane) with log₂fold change of 2 and a significance cut-off of $p < 0.01$ to assess the prevalence of surface membrane proteins in the pool of enriched proteins. Finally, to compare between the ARID1A-WT and mutant cell lines i.e AGS, NUGC-4 vs SNU-1, SNU-5 and OCUM-1, we first found the common significantly enriched plasma membrane proteins (log₂FC > 2 and $p < 0.01$) between AGS and NUGC-4 and similarly between SNU-1, SNU-5 and OCUM-1. These common groups were then further plotted in Venn diagrams to identify unique and common significantly enriched plasma membrane proteins between ARID1A-WT and mutant cell lines.

2.7 ARID1A Overexpression Cell Lines

We used a lentivirus system to induce overexpression in three non-isogenic ARID1A-deficient gastric cancer cell lines - SNU-1, SNU-5 and OCUM-1. We used three different tetracycline-inducible plasmid constructs per cell line - Empty, LacZ and ARID1A- puro lentivirus plasmids (pLenti-puro)[84]. These plasmids contain a puromycin-resistant gene that acts as a selection marker to identify successfully infected cells from the non-infected cells. A kill curve was used to determine the lowest concentration of puromycin that would be needed to effectively kill all the live cells in a plate. 400k, 200k, and 100k cells were seeded in each of the wells in a 6-well plate for SNU-5, OCUM-1 and SNU-1 cells respectively and incubated for 24 hrs before titrating it with various

concentrations of puromycin (0.1 ug/mL, 0.5ug/mL, 1ug/mL, 2ug/mL and 5ug/mL). Cell viability was measured using CellTitreGlo in SNU-5 and SNU-1 whereas crystal violet staining was used for OCUM-1 cells. 1 million HEK293T cells were seeded in a 10 cm dishes (3 plates per construct- Empty, Vector & ARID1A) one day before transfection of HEK293T cells. The following day packaging plasmids (pMDL9-RRE, pRSV-REV, pMD2G-VSVG) were mixed with respective target plasmids and added to HEK293T cells. The culture media was changed early the next morning followed by incubating the cells for 48hr at 37°C and 5% CO₂. After incubation, the viral media was harvested and added to target cells. For adherent cells OCUM-1, the harvested viral media was added to 1 million cells seeded in a 10cm dish and left to incubate in 37°C and 5% CO₂ for 48hrs. For suspension cell lines SNU-1 and SNU-5 we followed a typical double spinfection method in which 3 million cells were seeded (1 million per well) per construct for each of the cell lines in a 12-well plate and the virus was added to these wells along with polybrene. These cells are then centrifuged for 1.5 hr at 2500 rpm in 32°C. After this the cells are left to incubate for 24 hrs and the process was repeated followed by incubating the cells for 48hrs. After this, the cells were pooled together and transferred to 6-well plates for selection by adding puromycin. Puromycin ensures the killing of all the non-transfected cells. The cells are grown until confluency and then transferred to new flasks with fresh media and grown followed by doxycycline addition. Finally, we conducted a western blot to check for overexpression in the target cells.

2.8 RNA-Sequencing Analysis

Data for gastric cancer was downloaded from TCGA database-TCGA STAD (Stomach adenocarcinoma) and STAR counts analysed and normalised using DEseq2. 111 of the 412 samples were known to have ARID1A mutations. We further categorised these mutations on the basis of mutation types as truncating (frameshift, deletions and splice variants) or missense. Additionally, the tumour purity score was used to further normalise the gene counts according to the overall ARID1A expression in the tumour. Based on the PUREE calculation method, our TCGA-STAD samples purity scores ranged from 0.48 to 0.96, with an average score of 0.70. The Differentially expressed genes (DEGs) with expression values greater than $\log_2(0.5)$ and p-values < 0.05 were considered significantly upregulated or downregulated. The volcano plots showing the DEGs were generated using R-software. After Differential Gene Expression Analysis, pathway analysis was conducted using ClusterProfiler. Enriched pathways were selected using GO ontology for Cellular Compartments, Biological Process and Molecular Function. Statistically significant pathways were selected based on FDR values.

Chapter 3

Results

3.1 Cell-surface proteins can be efficiently enriched using Biotin-Streptavidin interaction

A frequently utilized method for investigating the cell surface proteome involves the addition of a biotin tag to the sugar chains of membrane glycoproteins or to extracellular lysine residues, followed by an extraction via pulldown using streptavidin analogs [50,51]. In our study, we used sulfo-NHS-SS-biotinylation followed by a pull-down using streptavidin dynabeads. Amongst the various biotinylation reagents present, Sulfo NHS-SS-Biotin has proven to show the best efficacy in isolating cell-surface molecules [52]. Its distinguishing features include the presence of a sulphonate group on the N-hydroxysuccinamide (NHS) ring which increases the water solubility of NHS-esters. Being hydrophilic makes it difficult for it to penetrate the plasma membrane, hence making it ideal for binding to cell-surface proteins. Chemically, sulfo-NHS esters react spontaneously with a deprotonated amine forming an amide bond (Fig.3).

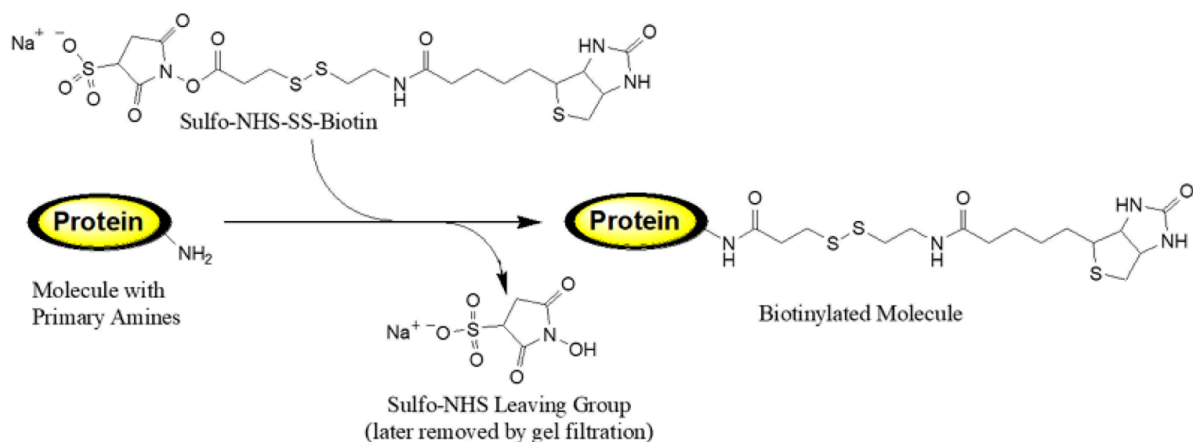


Figure 3. Structure of sulfo-NHS-SS-biotin molecule and its mechanism of action.

We first optimised this protocol for our gastric cancer (GC) cell lines by titrating the cells using different concentrations of biotin (0.5 mg/mL and 0.25 mg/mL) solution followed by a flow-cytometry analysis to confirm biotin tagging in the cells (Fig.5). We observed distinct peaks between the control samples and biotinylated samples in both the concentrations. Further, an IFA against a known cell-surface marker EGFR also confirmed the efficient binding of the biotin tags to

surface molecules (Fig.6). After optimization, we finally decided to use a concentration of 0.5mg/mL for our further experiments.

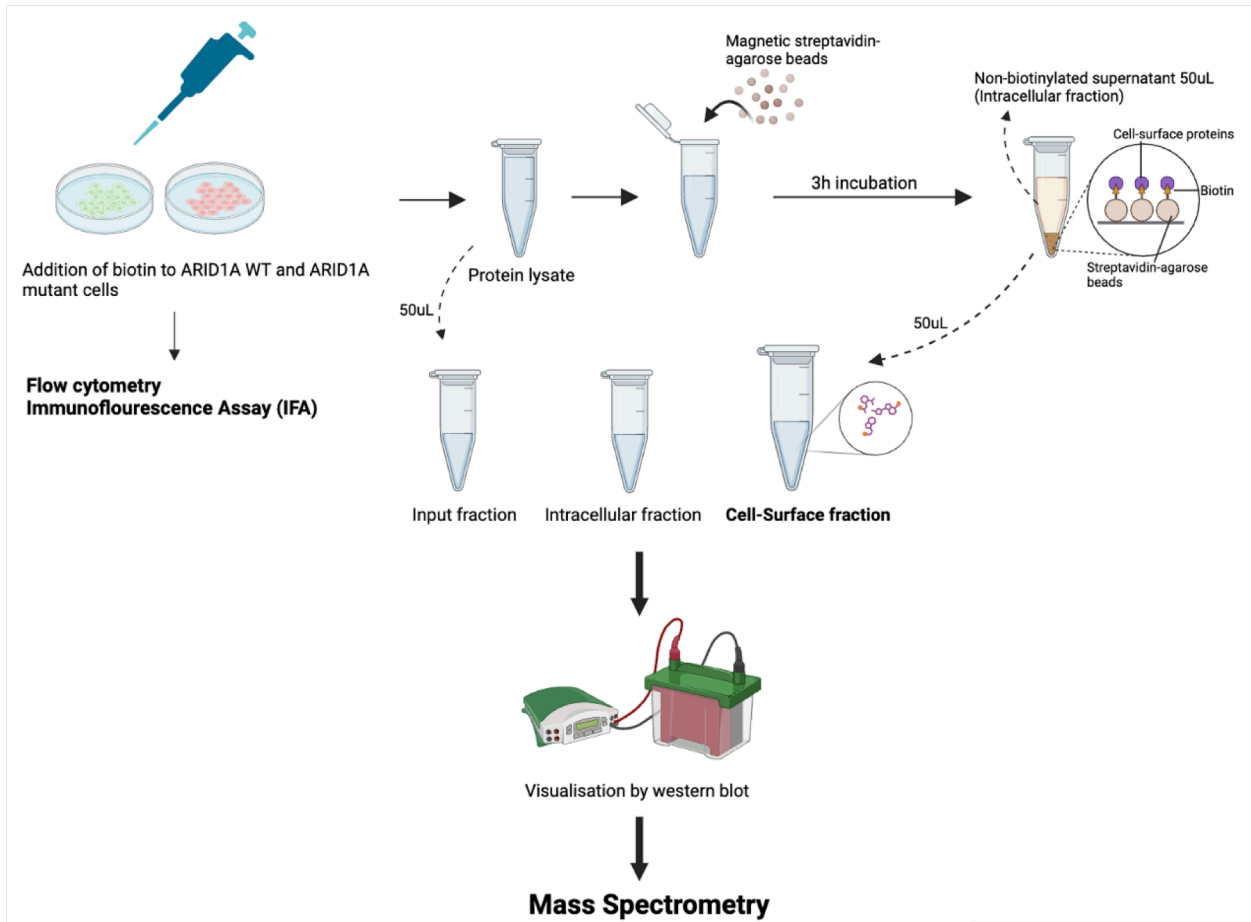


Figure 4. Overall methodology of cell-surface protein isolation and identification. (created by Biorender.com)

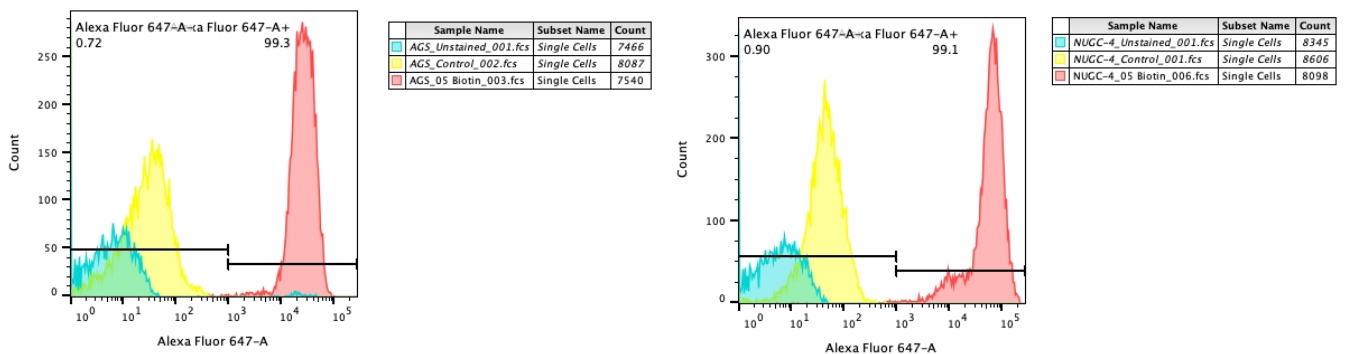


Figure 5. Flow-cytometry - Fluorescence peaks indicating biotinylated (red), non-biotinylated control (yellow) and unstained samples (blue). Figures a & b represent the following peaks at 0.5 mg/mL concentration of biotin solution in AGS and NUGC-4 cell lines respectively. (N=1, n=1)

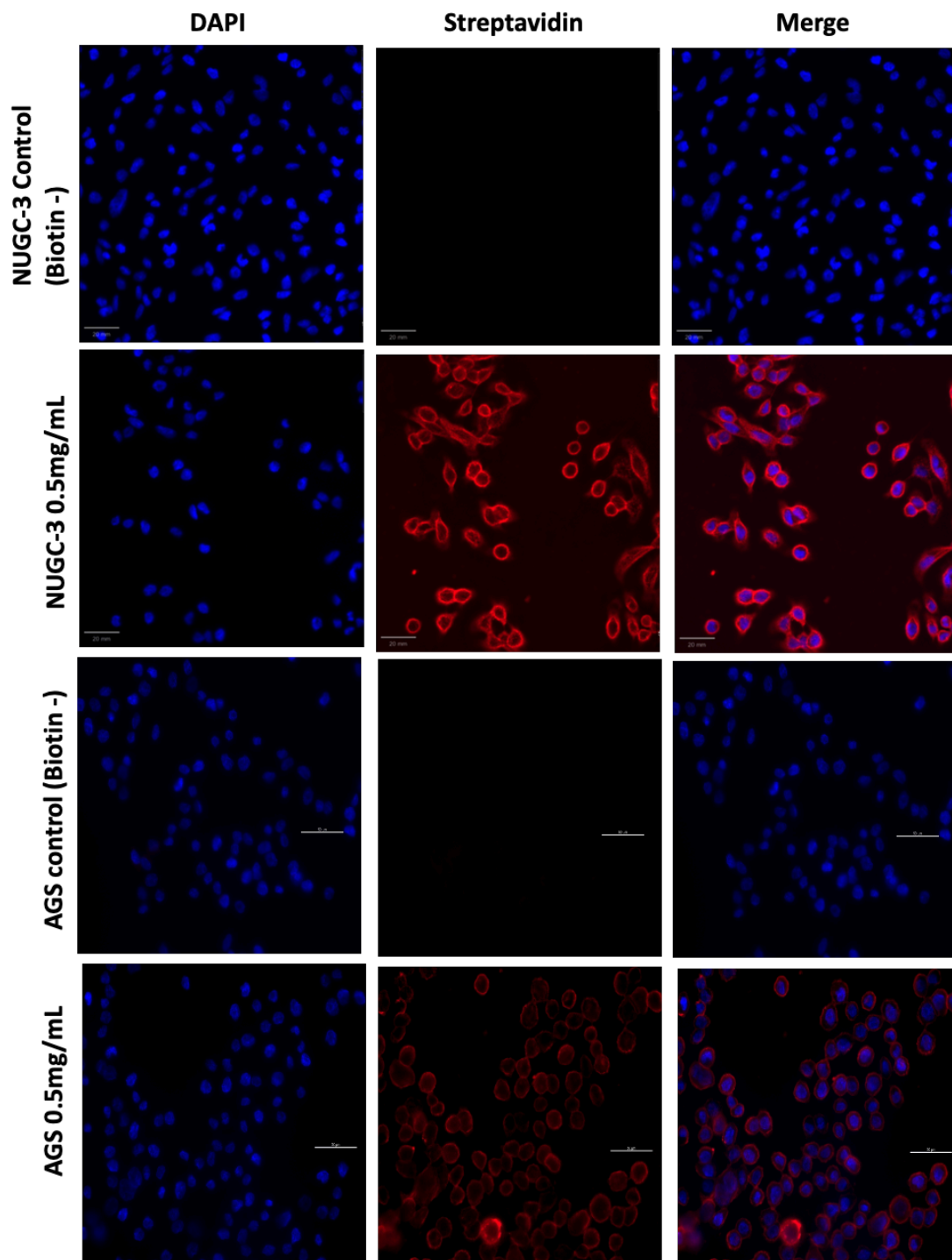


Figure 6. Fluorescence images AGS and NUGC-3 at 0.5 mg/mL biotin solution. (N=1, n=3)

Before our final optimisations, we also confirmed the expression of ARID1A in 10 GC cell lines using western blotting. AGS, HGC-27, NUGC-4, SNU-16 and KATO-III are ARID1A-WT whereas SNU-1,

SNU-5, NUGC-3, IM95 and OCUM-1 are ARID1A-mutant cell lines with SNU-1, SNU-5 and OCUM-1 showing complete lack ARID1A protein (Fig.7).

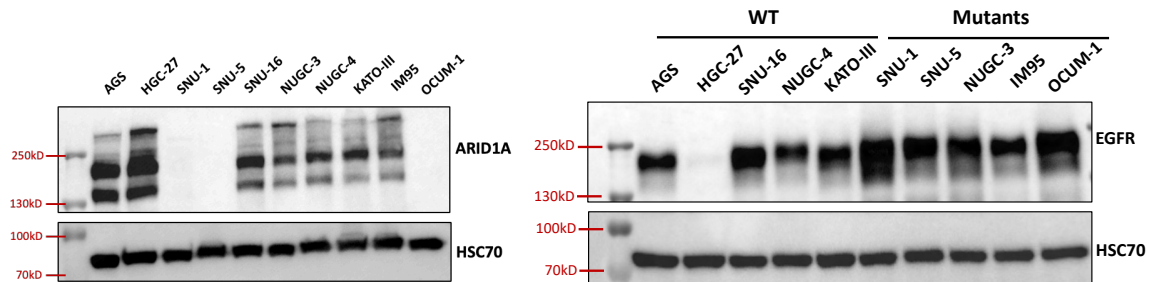


Figure 7. ARID1A & EGFR expression in ten different gastric cancer cell lines - ARID1A WT (AGS, HGC-27, SNU-16, KATO III, NUGC-4) and ARID1A mutants (SNU-1, SNU-5, NUGC-3, OCUM-1, IM95). Western blot analysis showed absence of ARID1A expression in SNU-1, SNU-5 and OCUM-1 cells (ARID1A mutants). The proteins were run on a 7% acrylamide gel for SDS-PAGE.

Prior to sending our samples for MS analysis we checked the pull-down results using western blotting (Fig.8). The western blots were used to compare the 'input' fraction containing all the cellular proteins including biotinylated membrane proteins as well as the other cytosolic proteins, the 'flow-through' or the 'intracellular' fraction which is the supernatant after incubating the lysate with streptavidin beads. This usually contains most of the cellular proteins excluding the plasma membrane and lastly, the 'cell-surface' fraction containing all the pulled-down proteins. All the 5 cell lines were appropriately tagged and the enriched proteins could be visualised using streptavidin-HRP in the western blots. For these, cytosolic protein B-actin was our negative control and as expected it always showed up in the input and flow-through fractions but never in the cell-surface fraction. On the other hand, EGFR was used as a positive control due to its usual presence on the plasma membrane. Fainter bands of EGFR in the cell-surface lane can be explained by the fact that cell-surface proteins comprise only a small part of the total proteins in the cell therefore, the concentration of proteins in the cell-surface is much less than the other lanes. Moreover, compared to the normal Laemmli buffer (containing DTT) used for elution of proteins from the beads for MS, the beads for the western blot were eluted only using Nu-PAGE 4X buffer (no DTT) because DTT acts as a reducing agent to break S-S bond in the biotin molecule rendering it unable to bind to streptavidin-HRP and hence no visual bands in the blot. Therefore, we can assume that the Nu-PAGE buffer is less efficient in eluting the proteins from the beads compared to the Laemmli buffer.

The enrichment analysis between the input, flow-through and the extracellular fraction using mass spectrometry confirmed the efficacy of the pull-down (Supplementary fig.2). We used a GO term analysis to see the relative abundance of cell surface and plasma membrane proteins compared to other proteins in the cells. In the plots below the pull-down proteins have been called the biotinylated group for simplicity. In all the 5 cell lines the biotinylated proteins always enriched for cell-surface proteins when compared to the input or the non-biotinylated fractions signifying the efficiency of our protocol and purity of our samples (Fig.9). In addition to this, a different plot comparing the enrichment between the 'input and biotinylated' as opposed to 'biotinylated vs input' proteins showed enrichment for other cytosolic and nuclear proteins further solidifying our claims.

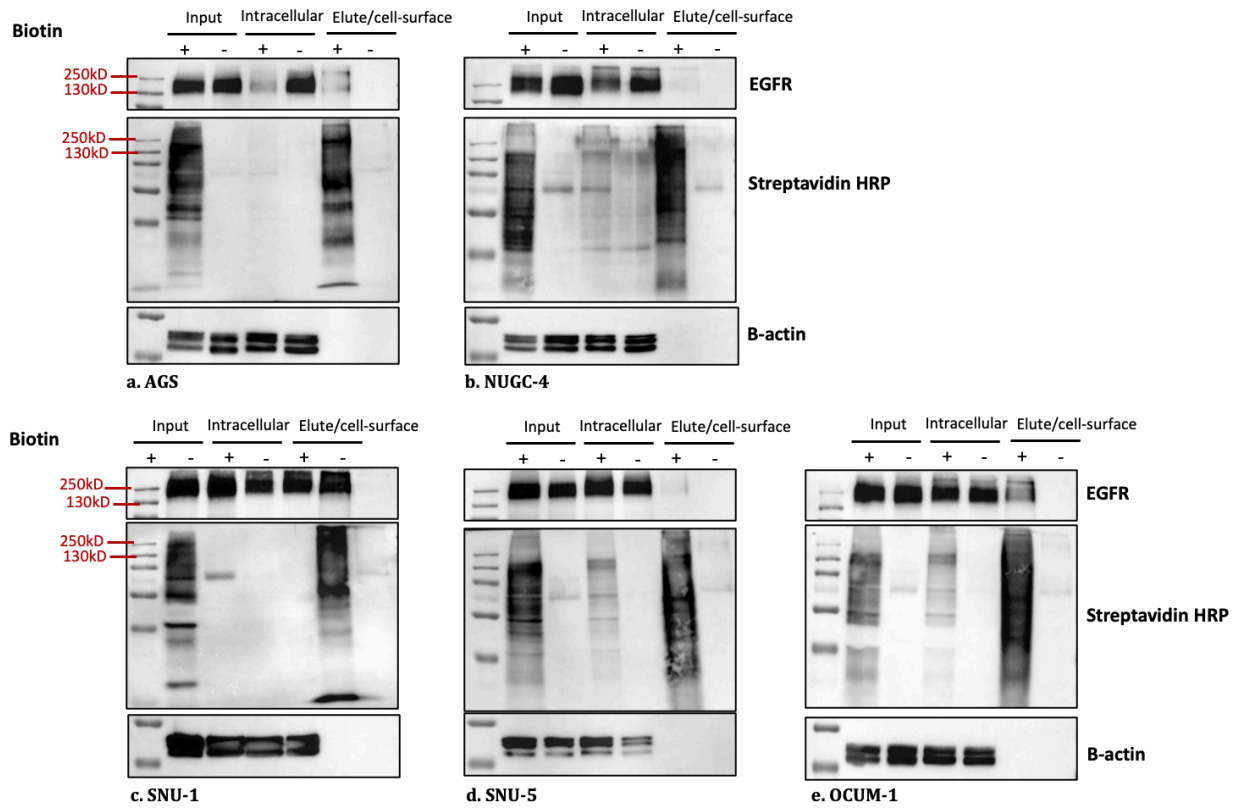
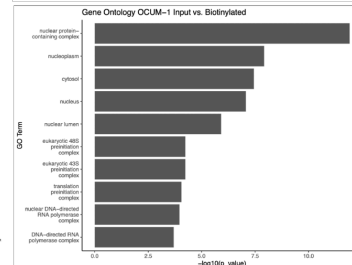
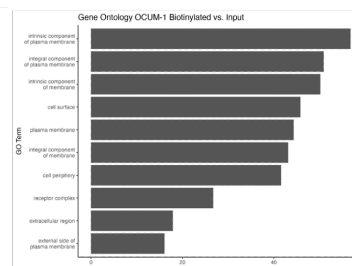
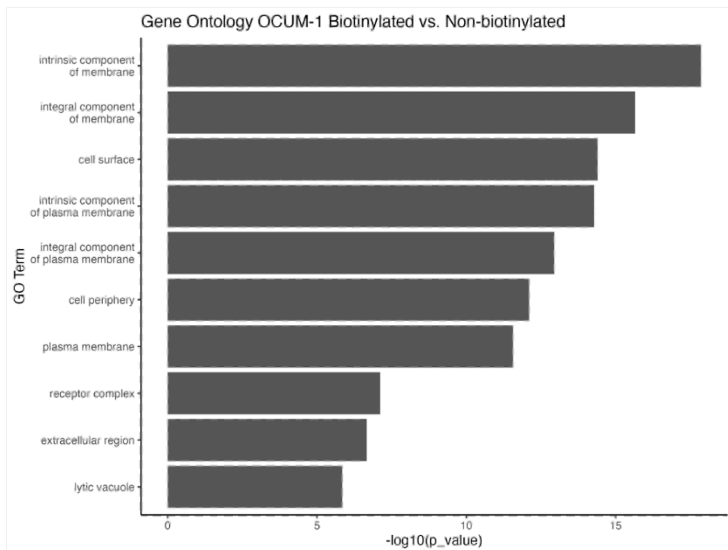
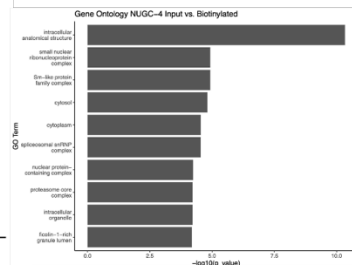
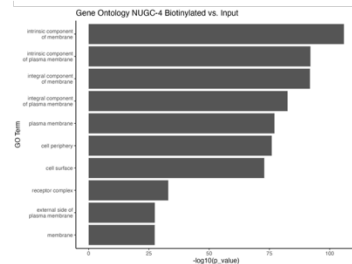
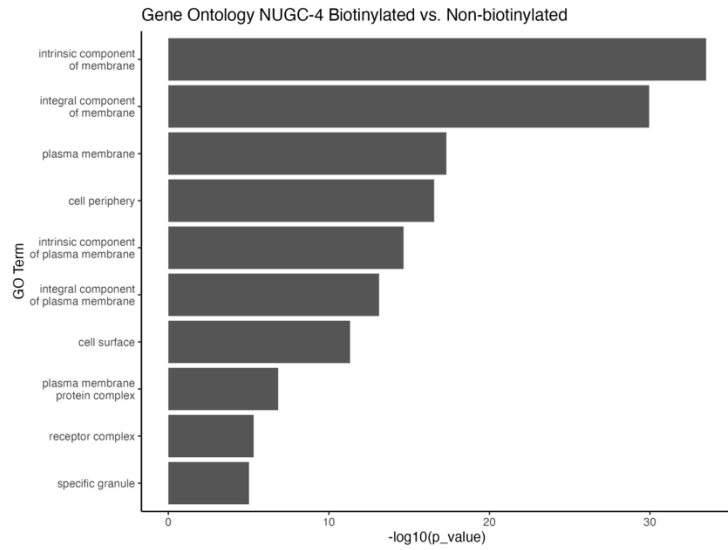
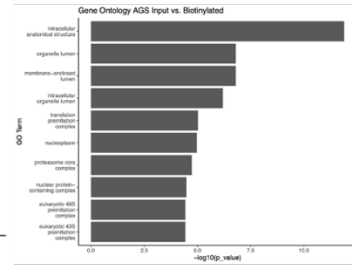
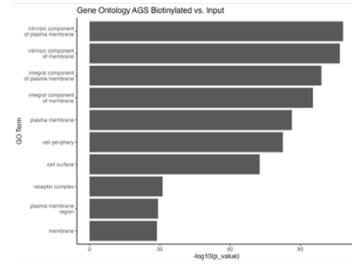
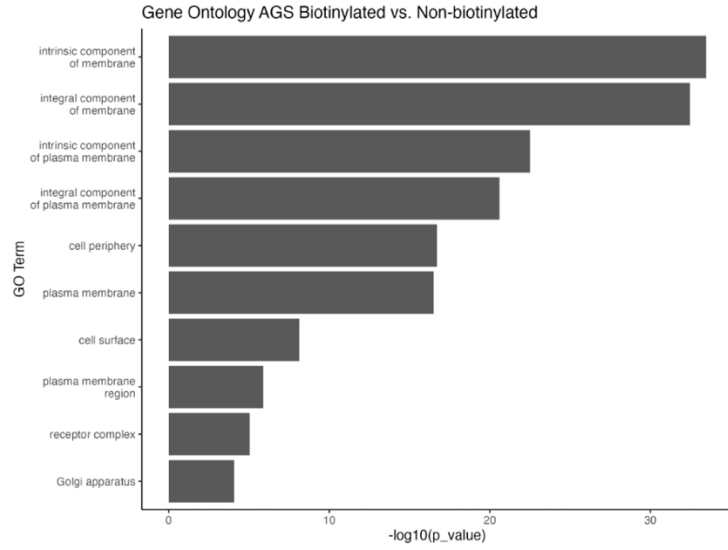


Figure 8. Biotin-streptavidin pull-down validation - Western blot confirming effective binding and isolation of the cell-surface proteins. The proteins were run on a 10% acrylamide gel for SDS-PAGE. (N=4 for each cell line)



these genes include calmodulin-2(CALM2), Annexin-1 (ANXA1), ezrin (EZR), macrophage migration inhibition factor (MIF), scavenger receptor protein class B member 2 (SCARB2), metadherin (MTDH), cell division cycle -42 (CDC42), RAC1 and actin related protein 2/3 complex subunit 2 (ARPC2) amongst the many others (Supplementary Figure 3). The major functions of some of these genes have been briefly mentioned subsequently.

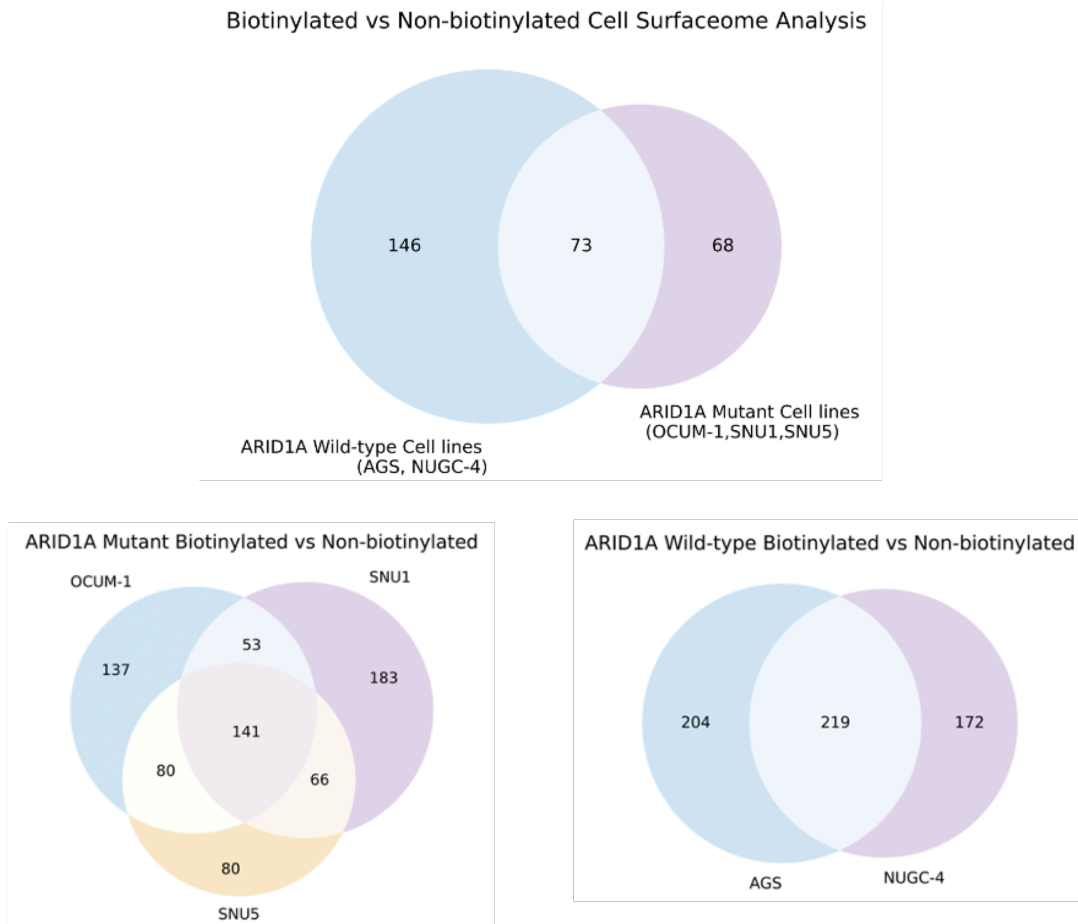


Figure 10. Venn diagrams show the number of unique and common proteins that were enriched in the biotinylated groups compared to the non-biotinylated controls in ARID1A-mutant & ARID1A-wt cell lines. The common surface proteins in the ARID1A-wt (219) and mutant groups (141) were then compared to find the unique and common cell-surface proteins between the two groups.

Calmodulin (CALM) is a Ca^{2+} binding protein existing in all eukaryotic cells. It can bind to various target proteins to manipulate the activities of multiple enzymes. It can also moderate control in various pathways and adaptor molecules that can have numerous downstream effects, hence controlling tumour cells' migration and invasion. Elevated expression of CALM2 has been associated with adverse prognostic outcomes in GC and has been shown to promote tumour cell proliferation, migration, invasion and angiogenesis in HUVEC cells. Moreover, CALM2 upregulation induces M2 polarisation of THP1 macrophage cells, contributing to the establishment of an immunosuppressive tumour microenvironment. In vivo models have demonstrated heightened

malignancy and metastasis in response to CALM2 upregulation. Mechanistically, it is believed to activate these pathways via the JAK2/STAT3/HIF-1/VEGFA axis in GC [54].

Annexin A1 (ANXA1) is a member of the calcium/phospholipid-binding protein family and is involved in various biological processes such as calcium signalling, anti-inflammatory effects, receptor mobilization, cell proliferation, and tumour progression. Its role in oncogenic functions including chemotaxis, invasion, and angiogenesis has been well documented [55]. In HER+ breast cancer, loss of ARID1A has been linked to resistance to Trastuzumab and promotion of metastasis through ANXA1 overexpression[56]. Similarly, in gastric cancer, increased ANXA1 expression is associated with advanced disease stages and peritoneal dissemination. It has been proposed that ANXA1 in GC transcriptionally upregulates membrane formyl peptide receptors (FPRs), leading to the activation of ITGB1BP1 via ERK phosphorylation. Additionally, ANXA1 contributes to an immunosuppressive microenvironment through mechanisms such as M2 polarization of macrophages and suppression of T-cell response[57].

Ezrin, a member of the ERM family of proteins regulates cell networks by linking actin cytoskeleton to the cell membranes [58]. The ERM family, actin cytoskeleton, and cell membranes collectively form dynamic domains like lamellipodia and filopodia, aiding in cell locomotion. ERM family proteins undergo regulated conformational changes between inactive and active states to engage with their interacting partners, a process tightly regulated by phosphorylation mediated by various kinases, including threonine and tyrosine kinases. Ezrin upregulation in the plasma membrane is usually associated with disruption of cell-cell contacts therefore facilitating the process of invasion. It is also responsible for controlling apical-basal polarity in normal cells [59]. Interestingly, ezrin was found to be significantly upregulated in most ARID1A-mutant cases and associated with unfavourable clinical outcomes in GC patients. Moreover, it was also observed to influence the tumour immune microenvironment with a notable positive correlation with neutrophil infiltration [60].

Another recent study directly highlights the role of P4HB in creating an immunosuppressive TME by activating cancer-associated fibroblasts (CAFs) in ARID1A-deficient lung cancer cells [53]. The exact mechanism of action remains elusive but P4HB is known to help in creating an oxidising environment in the endoplasmic reticulum (ER) for disulphide bond formation [63].

Along with the mentioned upregulated proteins, we observed the presence of several Rho-GTPases that have prominent and established roles in promoting and activating oncogenic pathways in multiple cancers [64]. Amongst the enriched proteins on ARID1A-deficient cells, Rho-GTPase family members CDC42 and RAC-1 are notably important regulators of tumour progression. Both of these have been shown to regulate multiple oncogenic pathways in cancer and influencing processes like metastasis by controlling microtubule instability, actin dynamics, transcription and nuclear signalling. RAC-1 responds to extracellular cues from hormones, adhesion molecules, cytokines and growth factors by alternating between an inactive GDP-bound form and an active GTP-bound form which is mediated by GAPs and GEFs [65]. Likewise, CDC42 also acts as a signal transducer whose activity is also regulated by guanine nucleotide exchange factors (GEFs) and GTPase-activating proteins (GAPs) and momentarily interacts with its downstream effector proteins eliciting cytoskeleton reorganisation, alterations in cell-cycle and transcription [66]. In addition, significant enrichment of several structural actin-cytoskeleton proteins like ARPC2 that have been well implicated in metastasis not only in GC but also other cancers[83] might point towards a role of ARID1A in indirectly controlling the actin dynamics and metastasis.

3.3 RNA-seq analysis further validated the role of immunosuppressive modulators in ARID1A-deficient Gastric Cancer patients

For further comprehensive understanding and validation of the enriched proteins in our proteomic analysis, we did an RNAseq analysis of 412 samples from the TCGA-STAD dataset. Our primary goal was to compare the differentially expressed genes (DEG) between ARID1A-mutant and ARID1A-WT patients. Amongst the 412 patient samples, 112 patients belonged to the ARID1A-mutant group whereas 300 samples belonged to the ARID1A-WT group. Ongoing studies in our lab using patient tissue samples from two distinct GC cohorts report a clear demarcation in the protein expression levels of ARID1A in the tumour cells compared to the surrounding stromal cells. Tumours with low ARID1A expression only show loss of ARID1A expression in the tumour cells, and not the stromal cells (Supplementary fig.4). In addition, we found that several tumours showed a higher presence of ARID1A despite being ARID1A-mutants, alluding to the fact that the ARID1A mutational status doesn't necessarily coincide with the protein expression. To account for these confounding variables, we used the tumour purity score to designate new count values for ARID1A expression in each patient. A higher tumour purity score would signify that the observed gene expression is primarily from the tumour core and the contrary would correspond to a higher stromal gene expression. Furthermore, we sub-divided the TCGA mutant group based on mutation type as truncating mutant variants (93/412) (Supplementary fig.5) and missense variants (19/412) for individual comparison of DEGs between the two groups against the wild-type (300/412) cases. Finally, we did a cohort-wide global comparison between all 412 samples based on overall ARID1A gene expression as ARID1A-low (gene expression <10.5) and ARID1A-high (gene expression > 12) (Fig 11 & 12).

We found many genes significantly upregulated genes in the ARID1A-low group among which six genes were common between our proteomic and transcriptomic analysis that included MIF, ANXA-1, SDHB, ARPC2, CSNK2B and NDUFC2.

Macrophage migration factor or MIF is a pleiotropic cytokine that inhibits the random migration of macrophages and is involved in the regulation of several immune and inflammatory processes[67]. MIF expression has now been shown to be elevated in multiple solid cancers and is generally correlated with a poorer prognosis [68]. Its oncogenic functions are facilitated by both autocrine and paracrine signalling which leads to various downstream effector pathways including the PIK3/AKT and the canonical ERK/ MAPK pathway in tumours, as well as immune cells like T-cells, dendritic cells and macrophages. Tumour-derived MIF stimulates myeloid-derived tumour suppressor (MDSCs) phenotype by its direct interaction with its receptor CD74 or via hetero-complexes like CD74/CXCR2 and CD74/CXCR4 or/and CXCR7. In addition, tumour-derived MIF causes tumour progression likely due to monocyte/macrophage-dependent angiogenesis and helping in M2 polarization of TAMs [69]. Alluding to this mechanism, we also found the significant upregulation of MIF, CD74, CXCR2 and CXCR4 (all p.adj < 0.001) in the ARID1A-low group.

Another notable moderator of immune function in our RNAseq analysis is indoleamine 2, 3-dioxygenase 1 or IDO-1. IDO-1 is a crucial cytosolic enzyme in the tryptophan catabolism pathway that converts tryptophan (Trp) to kynurenine (Kyn)[70]. The reduction of tryptophan levels and elevation of kynurenine play important roles in immune suppression by stimulating T-regulatory cells (Tregs) and MDSCs, compromising the function of effector T-cells and natural killer cells (NK cells), and promoting neovascularisation in solid tumours. Under normal physiological conditions in adult humans, IDO1 is typically absent in most tissues but is constitutively expressed in numerous types of cancer cells, stromal cells, and immune cells within the tumour

microenvironment. IDO-1 can be activated through several upstream pathways like IFN-gamma mediated JAK/STAT pathway, PI3K/PKC pathway, KIT/RAS and is also activated by immunomodulatory surface proteins like PD-L1 and CTLA-4 [71]. A recent study also reported increased tumour progression and immunosuppression in CD86 and PD-L1 positive hepatocellular carcinoma cells (HCC) through an IL-6/ISX (intestine-specific homeobox) axis [72]. Furthermore, extensive literature indicates a strong association of IDO-1 with resistance to immune checkpoint inhibitors (ICI) in multiple cancers [73]. Our cohort-wide analysis also showed a marked upregulation of PD-1 gene (PDCD1) in the ARID1A-low group. Currently, there are several ongoing clinical trials to devise effective combinatorial IDO-1 treatment options that improve response to ICI in solid tumours.

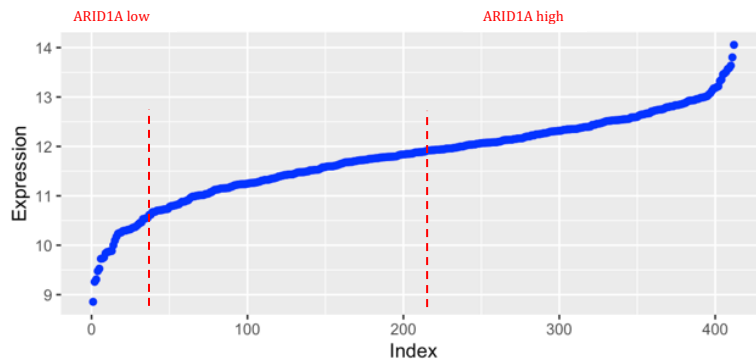


Figure 11. ARID1A gene expression plot – Figure shows ARID1A expression in 412 patients in the TCGA cohort with a median gene expression value of ~12 units. The ARID1A low and high cut-offs were made based on this expression pattern of ARID1A.

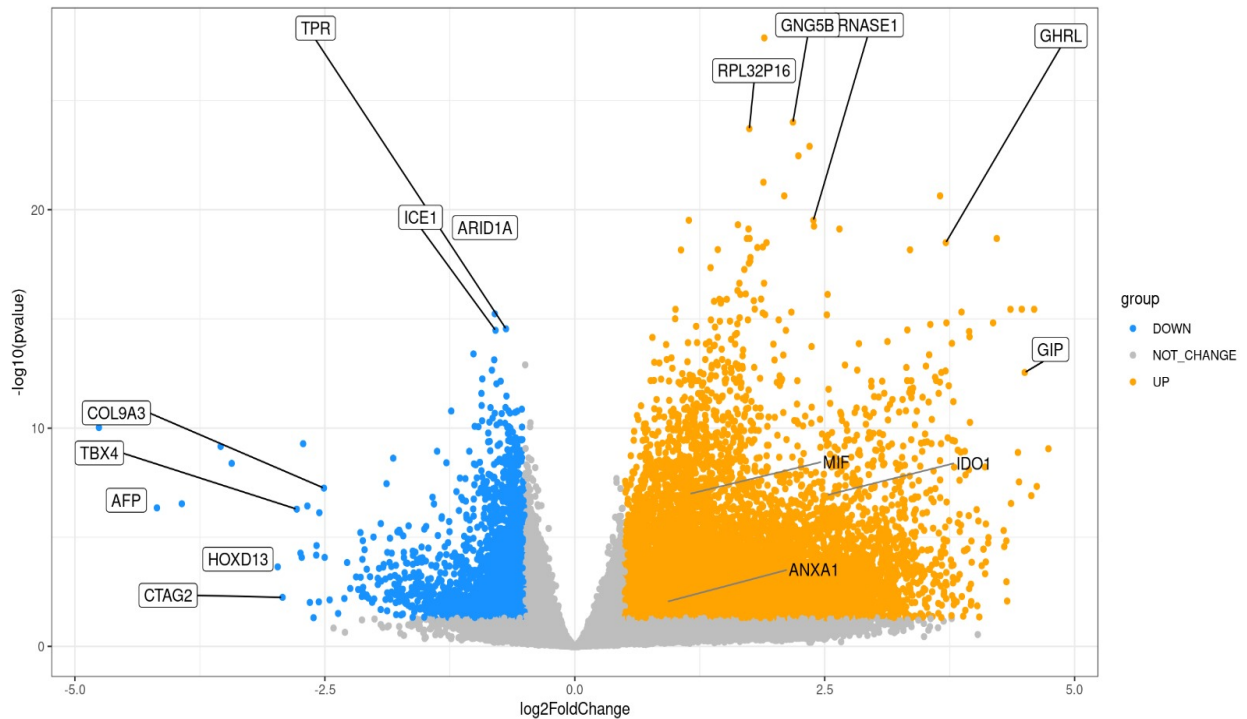


Figure 12. Volcano plot showing DEGs in ARID1A-high vs low tumours – Cut-off values for enriched proteins is value $>\log_2fc(0.5)$ and $p\text{-value} < 0.05$.

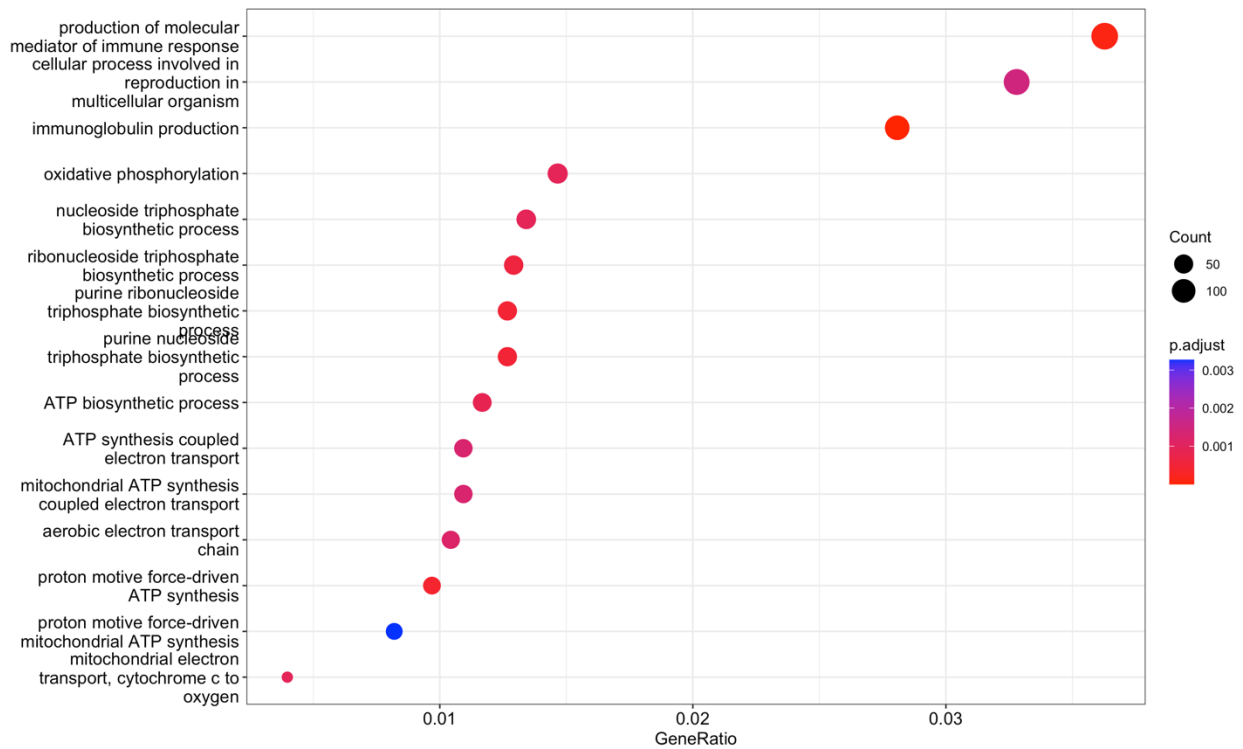


Figure 13. Enriched pathways in the DEGs between ARID1A-high vs low tumours

3.4 ARID1A and mitochondrial metabolism

Another frequently upregulated group of proteins we found include proteins that control cellular metabolism (SCRAB2, TKT, CRKL, etc), mitochondrial functions (SDHB, STOML2, VDAC-1, NDUFC2). (Fig.13 & Supplementary fig.3).

Previous data from lab has shown increased oxidative phosphorylation (OXPHOS) and mitochondrial depolarisation to be associated with ARID1A-deficiency in GC cell lines. These findings were further substantiated by the enrichment of mitochondrial OXPHOS genes at both the protein as well as RNA levels. SDHB, STOML2, VDAC-1 and NDUFC2 are known to have oncogenic functions in certain cancers [74,75,76], however deeper understanding of these genes in the context of ARID1A-deficiency remains to be elusive. Further analysis of the participating pathways involved would provide more meaningful conclusions to this observation.

Discussion

Being an important part of a chromatin remodeler, disruptions in the regular expression of ARID1A can lead to the altered functioning of the SWI/SNF complex leading to differential protein expression in the tumour cells. Despite the well-known implications of ARID1A-loss in tumour cells, there are currently no clinically relevant drugs to specifically target ARID1A-deficient cancers. This may be confounded by the heterogeneous nature of tumour cells and variability across different cancers. Moreover, surgical intervention and chemotherapy still remain to be the current norm for GC patients. Other treatment options like immunotherapy are usually used as a 2nd -3rd line treatment for GC patients with relatively low response rates [78]. Therefore, this compels us to look for new, safer and non-invasive combinatorial therapy options for at least a subset of GC patients with ARID1A deficiency.

Cell surface proteins play essential roles in immune responses, signalling pathways, cell interactions, and migration. Expression patterns of specific cell surface proteins are key determinants of cell identity and can be modified in various malignancies including cancer [77]. In cancer, these expression patterns can be regulated by several intrinsic and extrinsic factors that collectively influence the morphological, physiological and functional landscape of the tumour.

With this pretext, we compared the cell surfaceome of ARID1A-wt and deficient cells to examine differentially expressed proteins on the cell surface that might indicate possible targets for intervention. Our findings point towards an apparent correlation between ARID1A-loss and upregulation of surface proteins aiding in metastasis and invasion of cancer cells through diverse signalling cascades that control the tumour microenvironment (TME), cytoskeletal remodelling, cell survival and cell metabolism. A particular limitation to this was the limited number of cell lines that we could process in the given timeframe for our experiments. Other drawbacks to this are - i) asymmetrical comparison between the mutant and wildtype cell lines - 2 WT vs 3 mutant cell lines, ii) the cell lines were not similar in their source of origin - AGS cells come from a primary tumour whereas rest of the cell lines - NUGC-4, OCUM-1, SNU-1 & SNU-5 belong to metastatic tumours, iii) lastly, the WT cells (AGS & NUGC-4) were adherent cell lines and the mutant cell lines were primarily suspension cell lines (SNU-1, SNU-5) except OCUM-1 which was adherent. These differences may or may not cause a sizeable difference in our results, however, it is necessary to be mindful of these considerations.

Nevertheless, to further verify these results and look for additional targetable pathways, we did an *in-silico* analysis to compare the gene expression between ARID1A-high and low patients in the TCGA-STAD cohort of 412 cases. Six genes were found to be upregulated in both RNA-Seq and MS results - MIF, ANXA-1, SDHB, CSNK2B, NDUFC2 and ARPC2 between our proteomic and transcriptomic analysis. In addition, we also found IDO-1 as an important upregulated gene in ARID1A-low group in the RNA-seq analysis.

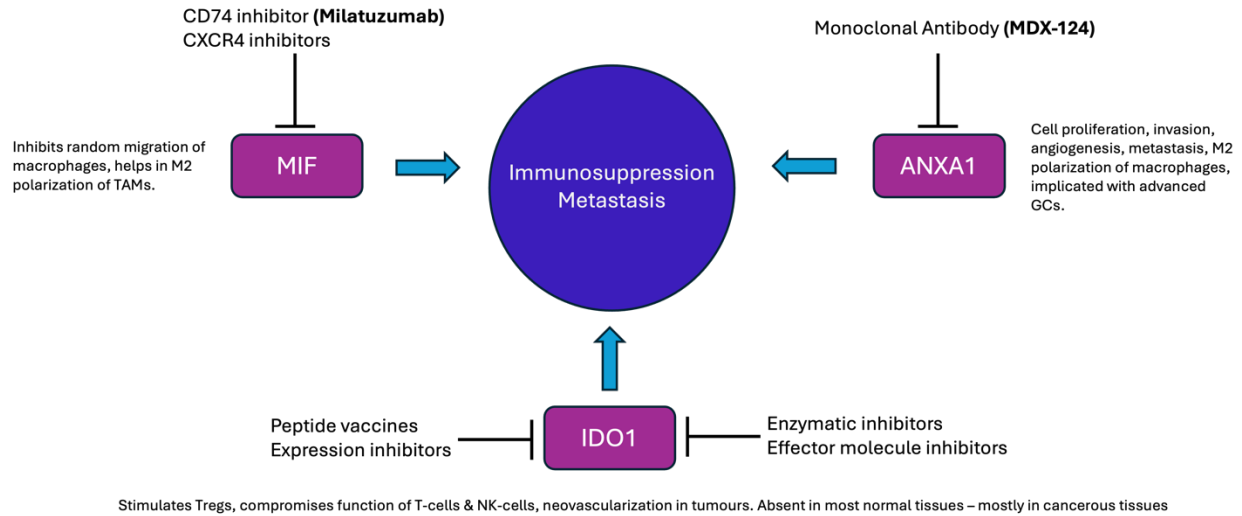


Figure.14 IDO-1, MIF and ANXA-1 can be possibly targeted using drugs to control immunosuppression and metastasis

ANXA-1 and IDO-1 are both well-characterized proteins with unambiguous and established roles in enabling an immunosuppressive TME which not only reduces the tumoricidal activation of the relevant immune cells but also facilitates metastasis and neovascularisation by the formation of a pro-tumorigenic inflammatory niche. Both of these genes have been implicated in immune responses that favour M2 macrophage polarization, and proliferation of MDSCs and Tregs by promoting enrichment in dendritic cells (DCs) and TH17 respectively. Recently, a humanised IgG1 monoclonal antibody (MDX-124) against ANXA1 showed a significant reduction in tumour growth in triple-negative breast cancer (TNBC) and pancreatic cancer syngeneic mouse models [79]. On the other hand, several enzymatic inhibitors for IDO-1 are currently under clinical trials with combination therapy with pembrolizumab, however, they have been halted due to unsatisfactory results [71].

As mentioned previously, MIF interacts with CD74 along with CXCR2/CXCR4/CXCR7 to induce M2 polarisation in TAMs and stimulate MDSCs. Even though this is widely known, MIF's functions in eliciting either pro- or anti-tumour responses in different effector cell types are many and are often context-dependent. However, it is believed that initially, MIF supports pro-inflammatory immune phenotypes during early events of tumorigenesis and recruits cells like macrophages and cytotoxic T-cells to restrain the tumour cells, however as the tumour growth progresses the MIF phenotype shifts towards wound resolution activities and MIF from both tumour cells and immune effector cells, transitions to instigating pro-tumorigenic immune evasion and neovascular processes across various immune cell types [69]. Our RNAseq analysis showed the presence of CD74, CXCR2 and CXCR4, which makes it an interesting avenue for drug intervention. Milatuzumab is an FDA-approved drug against CD74 for CLL and multiple myeloma [80]. Likewise, there are FDA-approved CXCR4 antagonists that are currently undergoing trials in combination with anti-PDL1 immunotherapy pembrolizumab for metastatic pancreatic ductal adenocarcinoma [81].

Taken together, our data suggests an apparent involvement of ARID1A in immunosuppression in the tumour and aggravating tumour proliferation and metastases (Fig.14). These findings align with the existing studies reporting the correlation between ARID1A loss and immunosuppressive

remodelling of the TME [32,82]. In addition to these similar observations, we report newer targets that have yet not been described in the context of ARID1A deficiency. In conclusion, we found that MIF, IDO-1 and ANXA1 are very good prospective drug targets from our initial preliminary analysis, which may have similar signalling pathways and might even have overlapping effector molecules. However, extensive downstream studies would be required to understand the functional, physiological and clinical implications associated with these proteins to make any definitive arguments.

References

- 1 Nair SS, Kumar R. Chromatin remodeling in cancer: a gateway to regulate gene transcription. *Mol Oncol*. 2012 Dec;6(6):611-9. doi: 10.1016/j.molonc.2012.09.005. Epub 2012 Oct 22. PMID: 23127546; PMCID: PMC3538127.
- 2 Wolffe, A. Chromatin remodeling: why it is important in cancer. *Oncogene* **20**, 2988–2990 (2001). <https://doi.org/10.1038/sj.onc.1204322>
- 3 Wang GG, Allis CD, Chi P. Chromatin remodeling and cancer, Part II: ATP-dependent chromatin remodeling. *Trends Mol Med*. 2007 Sep;13(9):373-80. doi: 10.1016/j.molmed.2007.07.004. Epub 2007 Sep 5. PMID: 17822959; PMCID: PMC4337864.
- 4 Shain AH, Pollack JR. The spectrum of SWI/SNF mutations, ubiquitous in human cancers. *PLoS One*. 2013;8(1):e55119. doi: 10.1371/journal.pone.0055119. Epub 2013 Jan 23. PMID: 23355908; PMCID: PMC3552954.
- 5 Kadoch C, Hargreaves DC, Hodges C, Elias L, Ho L, Ranish J, Crabtree GR. Proteomic and bioinformatic analysis of mammalian SWI/SNF complexes identifies extensive roles in human malignancy. *Nat Genet*. 2013 Jun;45(6):592-601. doi: 10.1038/ng.2628. Epub 2013 May 5. PMID: 23644491; PMCID: PMC3667980.
6. Mittal P, Roberts CWM. The SWI/SNF complex in cancer - biology, biomarkers and therapy. *Nat Rev Clin Oncol*. 2020 Jul;17(7):435-448. doi: 10.1038/s41571-020-0357-3. Epub 2020 Apr 17. PMID: 32303701; PMCID: PMC8723792.
7. Wu JN, Roberts CW. ARID1A mutations in cancer: another epigenetic tumor suppressor? *Cancer Discov*. 2013 Jan;3(1):35-43. doi: 10.1158/2159-8290.CD-12-0361. Epub 2012 Dec 3. PMID: 23208470; PMCID: PMC3546152.
8. Wang K, Kan J, Yuen ST, Shi ST, Chu KM, Law S, Chan TL, Kan Z, Chan AS, Tsui WY, Lee SP, Ho SL, Chan AK, Cheng GH, Roberts PC, Rejto PA, Gibson NW, Pocalyko DJ, Mao M, Xu J, Leung SY. Exome sequencing identifies frequent mutation of ARID1A in molecular subtypes of gastric cancer. *Nat Genet*. 2011 Oct 30;43(12):1219-23. doi: 10.1038/ng.982. PMID: 22037554.
9. Guichard C, Amaddeo G, Imbeaud S, Ladeiro Y, Pelletier L, Maad IB, Calderaro J, Bioulac-Sage P, Letexier M, Degos F, Clément B, Balabaud C, Chevet E, Laurent A, Couchy G, Letouzé E, Calvo F, Zucman-Rossi J. Integrated analysis of somatic mutations and focal copy-number changes identifies key genes and pathways in hepatocellular carcinoma. *Nat Genet*. 2012 May 6;44(6):694-8. doi: 10.1038/ng.2256. PMID: 22561517; PMCID: PMC3819251.
10. Mamo A, Cavallone L, Tuzmen S, Chabot C, Ferrario C, Hassan S, Edgren H, Kallioniemi O, Aleynikova O, Przybytkowski E, Malcolm K, Mousset S, Tonin PN, Basik M. An integrated genomic approach identifies ARID1A as a candidate tumor-suppressor gene in breast cancer. *Oncogene*. 2012 Apr 19;31(16):2090-100. doi: 10.1038/onc.2011.386. Epub 2011 Sep 5. PMID: 21892209.
11. Shain AH, Giacomini CP, Matsukuma K, Karikari CA, Bashyam MD, Hidalgo M, Maitra A, Pollack JR. Convergent structural alterations define SWItch/Sucrose NonFermentable (SWI/SNF) chromatin remodeler as a central tumor suppressive complex in pancreatic cancer. *Proc Natl Acad Sci U S A*. 2012 Jan 31;109(5):E252-9. doi: 10.1073/pnas.1114817109. Epub 2012 Jan 10. PMID: 22233809; PMCID: PMC3277150.

12. Gui Y, Guo G, Huang Y, Hu X, Tang A, Gao S, Wu R, Chen C, Li X, Zhou L, He M, Li Z, Sun X, Jia W, Chen J, Yang S, Zhou F, Zhao X, Wan S, Ye R, Liang C, Liu Z, Huang P, Liu C, Jiang H, Wang Y, Zheng H, Sun L, Liu X, Jiang Z, Feng D, Chen J, Wu S, Zou J, Zhang Z, Yang R, Zhao J, Xu C, Yin W, Guan Z, Ye J, Zhang H, Li J, Kristiansen K, Nickerson ML, Theodorescu D, Li Y, Zhang X, Li S, Wang J, Yang H, Wang J, Cai Z. Frequent mutations of chromatin remodeling genes in transitional cell carcinoma of the bladder. *Nat Genet.* 2011 Aug 7;43(9):875-8. doi: 10.1038/ng.907. PMID: 21822268; PMCID: PMC5373841.
13. Fantone S, Mazzucchelli R, Giannubilo SR, Ciavattini A, Marzioni D, Tossetta G. AT-rich interactive domain 1A protein expression in normal and pathological pregnancies complicated by preeclampsia. *Histochem Cell Biol.* 2020 Sep;154(3):339-346. doi: 10.1007/s00418-020-01892-8. Epub 2020 Jun 11. PMID: 32529396.
14. Wu RC, Wang TL, Shih IM. The emerging roles of ARID1A in tumor suppression. *Cancer Biol Ther.* 2014 Jun 1;15(6):655-64. doi: 10.4161/cbt.28411. Epub 2014 Mar 11. PMID: 24618703; PMCID: PMC4049780.
16. Suryo Rahmanto Y, Shen W, Shi X, Chen X, Yu Y, Yu ZC, Miyamoto T, Lee MH, Singh V, Asaka R, Shimberg G, Vitolo MI, Martin SS, Wirtz D, Drapkin R, Xuan J, Wang TL, Shih IM. Inactivation of ARID1A in the endometrium is associated with endometrioid tumorigenesis through transcriptional reprogramming. *Nat Commun.* 2020 Jun 1;11(1):2717. doi: 10.1038/s41467-020-16416-0. PMID: 32483112; PMCID: PMC7264300.
17. Lakshminarasimhan R, Andreu-Vieyra C, Lawrenson K, Duymich CE, Gayther SA, Liang G, Jones PA. Down-regulation of ARID1A is sufficient to initiate neoplastic transformation along with epigenetic reprogramming in non-tumorigenic endometriotic cells. *Cancer Lett.* 2017 Aug 10;401:11-19. doi: 10.1016/j.canlet.2017.04.040. Epub 2017 May 6. PMID: 28483516; PMCID: PMC5645058.
18. Reske JJ, Wilson MR, Holladay J, Siwicki RA, Skalski H, Harkins S, Adams M, Risinger JI, Hostetter G, Lin K, Chandler RL. Co-existing TP53 and ARID1A mutations promote aggressive endometrial tumorigenesis. *PLoS Genet.* 2021 Dec 23;17(12):e1009986. doi: 10.1371/journal.pgen.1009986. PMID: 34941867; PMCID: PMC8741038.
19. Mathur R, Alver BH, San Roman AK, Wilson BG, Wang X, Agoston AT, Park PJ, Shivdasani RA, Roberts CW. ARID1A loss impairs enhancer-mediated gene regulation and drives colon cancer in mice. *Nat Genet.* 2017 Feb;49(2):296-302. doi: 10.1038/ng.3744. Epub 2016 Dec 12. PMID: 27941798; PMCID: PMC5285448.
20. Baylin SB, Ohm JE. Epigenetic gene silencing in cancer - a mechanism for early oncogenic pathway addiction? *Nat Rev Cancer.* 2006 Feb;6(2):107-16. doi: 10.1038/nrc1799. PMID: 16491070.
21. Chandler RL, Damrauer JS, Raab JR, Schisler JC, Wilkerson MD, Didion JP, Starmer J, Serber D, Yee D, Xiong J, Darr DB, Pardo-Manuel de Villena F, Kim WY, Magnuson T. Coexistent ARID1A-PIK3CA mutations promote ovarian clear-cell tumorigenesis through pro-tumorigenic inflammatory cytokine signalling. *Nat Commun.* 2015 Jan 27;6:6118. doi: 10.1038/ncomms7118. PMID: 25625625; PMCID: PMC4308813.
25. Yamamoto S, Tsuda H, Takano M, Tamai S, Matsubara O. PIK3CA mutations and loss of ARID1A protein expression are early events in the development of cystic ovarian clear cell adenocarcinoma. *Virchows Arch.* 2012 Jan;460(1):77-87. doi: 10.1007/s00428-011-1169-8. Epub 2011 Nov 26. PMID: 22120431.
26. Bosse T, ter Haar NT, Seeber LM, v Diest PJ, Hes FJ, Vasen HF, Nout RA, Creutzberg CL, Morreau H, Smit VT. Loss of ARID1A expression and its relationship with PI3K-Akt pathway alterations, TP53 and microsatellite instability in endometrial cancer. *Mod Pathol.* 2013 Nov;26(11):1525-35. doi: 10.1038/modpathol.2013.96. Epub 2013 May 24. PMID: 23702729.
27. Rehman H, Chandrashekar DS, Balabhadrapatruni C, Nepal S, Balasubramanya SAH, Shelton AK, Skinner KR, Ma AH, Rao T, Agarwal S, Eich ML, Robinson AD, Naik G, Manne U, Netto GJ, Miller CR, Pan CX, Sonpavde G, Varambally S, Ferguson JE 3rd. ARID1A-deficient bladder cancer is dependent on PI3K signaling and sensitive

to EZH2 and PI3K inhibitors. *JCI Insight*. 2022 Aug 22;7(16):e155899. doi: 10.1172/jci.insight.155899. PMID: 35852858; PMCID: PMC9462490.

28. Fukumoto T, Park PH, Wu S, Fatkhutdinov N, Karakashev S, Nacarelli T, Kossenkov AV, Speicher DW, Jean S, Zhang L, Wang TL, Shih IM, Conejo-Garcia JR, Bitler BG, Zhang R. Repurposing Pan-HDAC Inhibitors for ARID1A-Mutated Ovarian Cancer. *Cell Rep*. 2018 Mar 27;22(13):3393-3400. doi: 10.1016/j.celrep.2018.03.019. PMID: 29590609; PMCID: PMC5903572.

29. Lewis EB. A gene complex controlling segmentation in *Drosophila*. *Nature*. 1978 Dec 7;276(5688):565-70. doi: 10.1038/276565a0. PMID: 103000.

30. Bitler BG, Aird KM, Garipov A, Li H, Amatangelo M, Kossenkov AV, Schultz DC, Liu Q, Shih IeM, Conejo-Garcia JR, Speicher DW, Zhang R. Synthetic lethality by targeting EZH2 methyltransferase activity in ARID1A-mutated cancers. *Nat Med*. 2015 Mar;21(3):231-8. doi: 10.1038/nm.3799. Epub 2015 Feb 16. PMID: 25686104; PMCID: PMC4352133.

32. Li J, Wang W, Zhang Y, Cieřlik M, Guo J, Tan M, Green MD, Wang W, Lin H, Li W, Wei S, Zhou J, Li G, Jing X, Vatan L, Zhao L, Bitler B, Zhang R, Cho KR, Dou Y, Kryczek I, Chan TA, Huntsman D, Chinnaiyan AM, Zou W. Epigenetic driver mutations in ARID1A shape cancer immune phenotype and immunotherapy. *J Clin Invest*. 2020 May 1;130(5):2712-2726. doi: 10.1172/JCI134402. PMID: 32027624; PMCID: PMC7190935.

33. 28 29 Shen J, Ju Z, Zhao W, Wang L, Peng Y, Ge Z, Nagel ZD, Zou J, Wang C, Kapoor P, Ma X, Ma D, Liang J, Song S, Liu J, Samson LD, Ajani JA, Li GM, Liang H, Shen X, Mills GB, Peng G. ARID1A deficiency promotes mutability and potentiates therapeutic antitumor immunity unleashed by immune checkpoint blockade. *Nat Med*. 2018 May;24(5):556-562. doi: 10.1038/s41591-018-0012-z. Epub 2018 May 7. PMID: 29736026; PMCID: PMC6076433.

34. Yakovlev VA. Nitric oxide-dependent downregulation of BRCA1 expression promotes genetic instability. *Cancer Res*. 2013 Jan 15;73(2):706-15. doi: 10.1158/0008-5472.CAN-12-3270. Epub 2012 Oct 29. PMID: 23108140; PMCID: PMC3549017.

35. Piscitello D, Varshney D, Lilla S, Vizioli MG, Reid C, Gorbunova V, Seluanov A, Gillespie DA, Adams PD. AKT overactivation can suppress DNA repair via p70S6 kinase-dependent downregulation of MRE11. *Oncogene*. 2018 Jan 25;37(4):427-438. doi: 10.1038/onc.2017.340. Epub 2017 Oct 2. PMID: 28967905; PMCID: PMC5799716.

36. Jia Y, Song W, Zhang F, Yan J, Yang Q. Akt1 inhibits homologous recombination in Brca1-deficient cells by blocking the Chk1-Rad51 pathway. *Oncogene*. 2013 Apr 11;32(15):1943-9. doi: 10.1038/onc.2012.211. Epub 2012 Jun 4. PMID: 22665067; PMCID: PMC3700338.

37. Plo I, Laulier C, Gauthier L, Lebrun F, Calvo F, Lopez BS. AKT1 inhibits homologous recombination by inducing cytoplasmic retention of BRCA1 and RAD51. *Cancer Res*. 2008 Nov 15;68(22):9404-12. doi: 10.1158/0008-5472.CAN-08-0861. PMID: 19010915.

38. Yakovlev VA, Sullivan SA, Fields EC, Temkin SM. PARP inhibitors in the treatment of ARID1A mutant ovarian clear cell cancer: PI3K/Akt1-dependent mechanism of synthetic lethality. *Front Oncol*. 2023 Feb 22;13:1124147. doi: 10.3389/fonc.2023.1124147. PMID: 36910637; PMCID: PMC9992988.

42. Zang ZJ, Cutcutache I, Poon SL, Zhang SL, McPherson JR, Tao J, Rajasegaran V, Heng HL, Deng N, Gan A, Lim KH, Ong CK, Huang D, Chin SY, Tan IB, Ng CC, Yu W, Wu Y, Lee M, Wu J, Poh D, Wan WK, Rha SY, So J, Salto-Tellez M, Yeoh KG, Wong WK, Zhu YJ, Futreal PA, Pang B, Ruan Y, Hillmer AM, Bertrand D, Nagarajan N, Rozen S, Teh BT, Tan P. Exome sequencing of gastric adenocarcinoma identifies recurrent somatic mutations in cell adhesion and chromatin remodeling genes. *Nat Genet*. 2012 May;44(5):570-4. doi: 10.1038/ng.2246. PMID: 22484628.

43. Abe H, Maeda D, Hino R, Otake Y, Isogai M, Ushiku AS, Matsusaka K, Kunita A, Ushiku T, Uozaki H, Tateishi Y, Hishima T, Iwasaki Y, Ishikawa S, Fukayama M. ARID1A expression loss in gastric cancer: pathway-dependent roles with and without Epstein-Barr virus infection and microsatellite instability. *Virchows Arch*. 2012 Oct;461(4):367-77. doi: 10.1007/s00428-012-1303-2. Epub 2012 Aug 23. PMID: 22915242.
44. Ashizawa M, Saito M, Min AKT, Ujiie D, Saito K, Sato T, Kikuchi T, Okayama H, Fujita S, Endo H, Sakamoto W, Momma T, Ohki S, Goto A, Kono K. Prognostic role of ARID1A negative expression in gastric cancer. *Sci Rep*. 2019 May 1;9(1):6769. doi: 10.1038/s41598-019-43293-5. PMID: 31043675; PMCID: PMC6494900.
45. Wu S, Fukumoto T, Lin J, Nacarelli T, Wang Y, Ong D, Liu H, Fatkhutdinov N, Zundell JA, Karakashev S, Zhou W, Schwartz LE, Tang HY, Drapkin R, Liu Q, Huntsman DG, Kossenkov AV, Speicher DW, Schug ZT, Van Dang C, Zhang R. Targeting glutamine dependence through GLS1 inhibition suppresses ARID1A-inactivated clear cell ovarian carcinoma. *Nat Cancer*. 2021 Feb;2(2):189-200. doi: 10.1038/s43018-020-00160-x. Epub 2021 Jan 11. PMID: 34085048; PMCID: PMC8168620.
46. Xiang L, Mou J, Shao B, Wei Y, Liang H, Takano N, Semenza GL, Xie G. Glutaminase 1 expression in colorectal cancer cells is induced by hypoxia and required for tumor growth, invasion, and metastatic colonization. *Cell Death Dis*. 2019 Jan 17;10(2):40. doi: 10.1038/s41419-018-1291-5. PMID: 30674873; PMCID: PMC6426853.
47. Srinivas US, Tay NSC, Jaynes P, Anbuselvan A, Ramachandran GK, Wardyn JD, Hoppe MM, Hoang PM, Peng Y, Lim S, Lee MY, Peethala PC, An O, Shendre A, Tan BWQ, Jemimah S, Lakshmanan M, Hu L, Jakhar R, Sachaphibulkij K, Lim LHK, Pervaiz S, Crasta K, Yang H, Tan P, Liang C, Ho L, Khanchandani V, Kappei D, Yong WP, Tan DSP, Bordi M, Campello S, Tam WL, Frezza C, Jeyasekharan AD. PLK1 inhibition selectively induces apoptosis in ARID1A deficient cells through uncoupling of oxygen consumption from ATP production. *Oncogene*. 2022 Mar;41(13):1986-2002. doi: 10.1038/s41388-022-02219-8. Epub 2022 Mar 2. Erratum in: *Oncogene*. 2022 Jun;41(24):3382. PMID: 35236967.
48. Ogiwara H, Takahashi K, Sasaki M, Kuroda T, Yoshida H, Watanabe R, Maruyama A, Makinoshima H, Chiwaki F, Sasaki H, Kato T, Okamoto A, Kohno T. Targeting the Vulnerability of Glutathione Metabolism in ARID1A-Deficient Cancers. *Cancer Cell*. 2019 Feb 11;35(2):177-190.e8. doi: 10.1016/j.ccell.2018.12.009. Epub 2019 Jan 24. PMID: 30686770.
49. Kirkemo LL, Elledge SK, Yang J, Byrnes JR, Glasgow JE, Blleloch R, Wells JA. Cell-surface tethered promiscuous biotinylators enable comparative small-scale surface proteomic analysis of human extracellular vesicles and cells. *Elife*. 2022 Mar 8;11:e73982. doi: 10.7554/eLife.73982. PMID: 35257663; PMCID: PMC8983049.
50. Wollscheid B, Bausch-Fluck D, Henderson C, O'Brien R, Bibel M, Schiess R, Aebersold R, Watts JD. Mass-spectrometric identification and relative quantification of N-linked cell surface glycoproteins. *Nat Biotechnol*. 2009 Apr;27(4):378-86. doi: 10.1038/nbt.1532. Epub 2009 Apr 6. Erratum in: *Nat Biotechnol*. 2009 Sep;27(9):864. PMID: 19349973; PMCID: PMC2829300.
51. Hörmann K, Stukalov A, Müller AC, Heinz LX, Superti-Furga G, Colinge J, Bennett KL. A Surface Biotinylation Strategy for Reproducible Plasma Membrane Protein Purification and Tracking of Genetic and Drug-Induced Alterations. *J Proteome Res*. 2016 Feb 5;15(2):647-58. doi: 10.1021/acs.jproteome.5b01066. Epub 2016 Jan 12. PMID: 26699813.
52. Huang R, Wu D, Zhang K, Hu G, Liu Y, Jiang Y, Wang C, Zheng Y. ARID1A loss induces P4HB to activate fibroblasts to support lung cancer cell growth, invasion, and chemoresistance. *Cancer Sci*. 2024 Feb;115(2):439-451. doi: 10.1111/cas.16052. Epub 2023 Dec 15. PMID: 38100120; PMCID: PMC10859615.

54. Mu G, Zhu Y, Dong Z, Shi L, Deng Y, Li H. Calmodulin 2 Facilitates Angiogenesis and Metastasis of Gastric Cancer *via* STAT3/HIF-1A/VEGF-A Mediated Macrophage Polarization. *Front Oncol.* 2021 Sep 15;11:727306. doi: 10.3389/fonc.2021.727306. PMID: 34604066; PMCID: PMC8479158.
55. Araújo TG, Mota STS, Ferreira HSV, Ribeiro MA, Goulart LR, Vecchi L. Annexin A1 as a Regulator of Immune Response in Cancer. *Cells.* 2021 Aug 30;10(9):2245. doi: 10.3390/cells10092245. PMID: 34571894; PMCID: PMC8464935.
56. Berns K, Sonnenblick A, Gennissen A, Brohée S, Hijmans EM, Evers B, Fumagalli D, Desmedt C, Loibl S, Denkert C, Neven P, Guo W, Zhang F, Knijnenburg TA, Bosse T, van der Heijden MS, Hindriksen S, Nijkamp W, Wessels LF, Joensuu H, Mills GB, Beijersbergen RL, Sotiriou C, Bernardis R. Loss of ARID1A Activates ANXA1, which Serves as a Predictive Biomarker for Trastuzumab Resistance. *Clin Cancer Res.* 2016 Nov 1;22(21):5238-5248. doi: 10.1158/1078-0432.CCR-15-2996. Epub 2016 May 12. PMID: 27172896.
57. Cheng TY, Wu MS, Lin JT, Lin MT, Shun CT, Huang HY, Hua KT, Kuo ML. Annexin A1 is associated with gastric cancer survival and promotes gastric cancer cell invasiveness through the formyl peptide receptor/extracellular signal-regulated kinase/integrin beta-1-binding protein 1 pathway. *Cancer.* 2012 Dec 1;118(23):5757-67. doi: 10.1002/cncr.27565. Epub 2012 Jun 26. PMID: 22736399.
58. Kong J, Li Y, Liu S, Jin H, Shang Y, Quan C, Li Y, Lin Z. High expression of ezrin predicts poor prognosis in uterine cervical cancer. *BMC Cancer.* 2013 Nov 4;13:520. doi: 10.1186/1471-2407-13-520. PMID: 24182314; PMCID: PMC4228363.
59. Song Y, Ma X, Zhang M, Wang M, Wang G, Ye Y, Xia W. Ezrin Mediates Invasion and Metastasis in Tumorigenesis: A Review. *Front Cell Dev Biol.* 2020 Nov 10;8:588801. doi: 10.3389/fcell.2020.588801. PMID: 33240887; PMCID: PMC7683424.
60. Zhu Y, Zhang X, Chen Y, Liu Q, Yang J, Fan X, Song H, Cheng Z, Liu S. Ezrin's role in gastric cancer progression: Implications for immune microenvironment modulation and therapeutic potential. *Heliyon.* 2024 Feb 28;10(5):e27155. doi: 10.1016/j.heliyon.2024.e27155. PMID: 38449647; PMCID: PMC10915575.
61. Hoyer J, Ekici AB, Ende S, Popp B, Zweier C, Wiesener A, Wohlleber E, Dufke A, Rossier E, Petsch C, Zweier M, Göhring I, Zink AM, Rappold G, Schröck E, Wiczorek D, Riess O, Engels H, Rauch A, Reis A. Haploinsufficiency of ARID1B, a member of the SWI/SNF-a chromatin-remodeling complex, is a frequent cause of intellectual disability. *Am J Hum Genet.* 2012 Mar 9;90(3):565-72. doi: 10.1016/j.ajhg.2012.02.007. PMID: 22405089; PMCID: PMC3309205.
62. Mullen J, Kato S, Sicklick JK, Kurzrock R. Targeting ARID1A mutations in cancer. *Cancer Treat Rev.* 2021 Nov;100:102287. doi: 10.1016/j.ctrv.2021.102287. Epub 2021 Sep 6. PMID: 34619527.
63. Feng D, Wang J, Li D, Wu R, Tuo Z, Yu Q, Ye L, Miyamoto A, Yoo KH, Wang C, Cheng Y, Ye X, Zhang C, Wei W. Targeting Prolyl 4-Hydroxylase Subunit Beta (P4HB) in Cancer: New Roads to Travel. *Aging Dis.* 2023 Nov 26. doi: 10.14336/AD.2023.1126. Epub ahead of print. PMID: 38029391.
64. Haga RB, Ridley AJ. Rho GTPases: Regulation and roles in cancer cell biology. *Small GTPases.* 2016 Oct;7(4):207-221. doi: 10.1080/21541248.2016.1232583. Epub 2016 Sep 14. PMID: 27628050; PMCID: PMC5129894.
65. Bosco EE, Mulloy JC, Zheng Y. Rac1 GTPase: a "Rac" of all trades. *Cell Mol Life Sci.* 2009 Feb;66(3):370-4. doi: 10.1007/s00018-008-8552-x. PMID: 19151919; PMCID: PMC6669905.
66. Xiao XH, Lv LC, Duan J, Wu YM, He SJ, Hu ZZ, Xiong LX. Regulating Cdc42 and Its Signaling Pathways in Cancer: Small Molecules and MicroRNA as New Treatment Candidates. *Molecules.* 2018 Mar 29;23(4):787. doi: 10.3390/molecules23040787. PMID: 29596304; PMCID: PMC6017947.

67. Guda MR, Rashid MA, Asuthkar S, Jalsutram A, Caniglia JL, Tsung AJ, Velpula KK. Pleiotropic role of macrophage migration inhibitory factor in cancer. *Am J Cancer Res*. 2019 Dec 1;9(12):2760-2773. PMID: 31911860; PMCID: PMC6943360.
68. Charan, M., Das, S., Mishra, S. *et al*. Macrophage migration inhibitory factor inhibition as a novel therapeutic approach against triple-negative breast cancer. *Cell Death Dis* **11**, 774 (2020). <https://doi.org/10.1038/s41419-020-02992-y>
69. Noe JT, Mitchell RA. MIF-Dependent Control of Tumor Immunity. *Front Immunol*. 2020 Nov 25;11:609948. doi: 10.3389/fimmu.2020.609948. PMID: 33324425; PMCID: PMC7724107.
70. Prendergast GC, Smith C, Thomas S, Mandik-Nayak L, Laury-Kleintop L, Metz R, Muller AJ. Indoleamine 2,3-dioxygenase pathways of pathogenic inflammation and immune escape in cancer. *Cancer Immunol Immunother*. 2014 Jul;63(7):721-35. doi: 10.1007/s00262-014-1549-4. Epub 2014 Apr 8. PMID: 24711084; PMCID: PMC4384696.
71. Liu M, Wang X, Wang L, Ma X, Gong Z, Zhang S, Li Y. Targeting the IDO1 pathway in cancer: from bench to bedside. *J Hematol Oncol*. 2018 Aug 2;11(1):100. doi: 10.1186/s13045-018-0644-y. PMID: 30068361; PMCID: PMC6090955.
72. Wang LT, Chiou SS, Chai CY, Hsi E, Yokoyama KK, Wang SN, Huang SK, Hsu SH. Intestine-Specific Homeobox Gene *ISX* Integrates IL6 Signaling, Tryptophan Catabolism, and Immune Suppression. *Cancer Res*. 2017 Aug 1;77(15):4065-4077. doi: 10.1158/0008-5472.CAN-17-0090. Epub 2017 Jun 16. PMID: 28625979.
73. Holmgaard RB, Zamarin D, Munn DH, Wolchok JD, Allison JP. Indoleamine 2,3-dioxygenase is a critical resistance mechanism in antitumor T cell immunotherapy targeting CTLA-4. *J Exp Med*. 2013 Jul 1;210(7):1389-402. doi: 10.1084/jem.20130066. Epub 2013 Jun 10. PMID: 23752227; PMCID: PMC3698523.
74. Saxena N, Maio N, Crooks DR, Ricketts CJ, Yang Y, Wei MH, Fan TW, Lane AN, Sourbier C, Singh A, Killian JK, Meltzer PS, Vocke CD, Rouault TA, Linehan WM. SDHB-Deficient Cancers: The Role of Mutations That Impair Iron Sulfur Cluster Delivery. *J Natl Cancer Inst*. 2016 Jan;108(1):djv287. doi: 10.1093/jnci/djv287. PMID: 26719882; PMCID: PMC4732025.
75. Igci YZ, Bozgeyik E, Borazan E, Pala E, Suner A, Ulasli M, Gurses SA, Yumrutas O, Balik AA, Igci M. Expression profiling of SCN8A and NDUFC2 genes in colorectal carcinoma. *Exp Oncol*. 2015 Mar;37(1):77-80. PMID: 25804238.
76. Li XH, He F, Yan SM, Li Y, Cao Y, Huang CY, Zhou ZW. Increased expression of stomatin-like protein 2 (STOML2) predicts decreased survival in gastric adenocarcinoma: a retrospective study. *Med Oncol*. 2014 Jan;31(1):763. doi: 10.1007/s12032-013-0763-9. Epub 2013 Nov 21. PMID: 24258357.
77. Garapati K, Ding H, Charlesworth MC, Kim Y, Zenka R, Saraswat M, Mun DG, Chavan S, Shingade A, Lucien F, Zhong J, Kandasamy RK, Pandey A. sBioSITE enables sensitive identification of the cell surface proteome through direct enrichment of biotinylated peptides. *Clin Proteomics*. 2023 Dec 5;20(1):56. doi: 10.1186/s12014-023-09445-6. PMID: 38053024; PMCID: PMC10696767.
78. Sexton RE, Al Hallak MN, Diab M, Azmi AS. Gastric cancer: a comprehensive review of current and future treatment strategies. *Cancer Metastasis Rev*. 2020 Dec;39(4):1179-1203. doi: 10.1007/s10555-020-09925-3. Epub 2020 Sep 7. PMID: 32894370; PMCID: PMC7680370.
79. Al-Ali HN, Crichton SJ, Fabian C, Pepper C, Butcher DR, Dempsey FC, Parris CN. A therapeutic antibody targeting annexin-A1 inhibits cancer cell growth in vitro and in vivo. *Oncogene*. 2024 Feb;43(8):608-614. doi: 10.1038/s41388-023-02919-9. Epub 2024 Jan 10. PMID: 38200229; PMCID: PMC10873194.

80. Haran M, Mirkin V, Braester A, Harpaz N, Shevetz O, Shtreiter M, Greenberg S, Mordich O, Amram O, Binsky-Ehrenreich I, Marom A, Shachar I, Herishanu Y, Ruchlemer R, Berrebi A, Valinsky L, Shtalrid M, Shvidel L. A phase I-II clinical trial of the anti-CD74 monoclonal antibody milatuzumab in frail patients with refractory chronic lymphocytic leukaemia: A patient based approach. *Br J Haematol.* 2018 Jul;182(1):125-128. doi: 10.1111/bjh.14726. Epub 2017 May 3. PMID: 28466956.
81. Bockorny B, Semenisty V, Macarulla T, Borazanci E, Wolpin BM, Stemmer SM, Golan T, Geva R, Borad MJ, Pedersen KS, Park JO, Ramirez RA, Abad DG, Feliu J, Muñoz A, Ponz-Sarvise M, Peled A, Lustig TM, Bohana-Kashtan O, Shaw SM, Sorani E, Chaney M, Kadosh S, Vainstein Haras A, Von Hoff DD, Hidalgo M. BL-8040, a CXCR4 antagonist, in combination with pembrolizumab and chemotherapy for pancreatic cancer: the COMBAT trial. *Nat Med.* 2020 Jun;26(6):878-885. doi: 10.1038/s41591-020-0880-x. Epub 2020 May 25. PMID: 32451495.
82. Li N, Liu Q, Han Y, Pei S, Cheng B, Xu J, Miao X, Pan Q, Wang H, Guo J, Wang X, Zhang G, Lian Y, Zhang W, Zang Y, Tan M, Li Q, Wang X, Xiao Y, Hu G, Jiang J, Huang H, Qin J. ARID1A loss induces polymorphonuclear myeloid-derived suppressor cell chemotaxis and promotes prostate cancer progression. *Nat Commun.* 2022 Nov 26;13(1):7281. doi: 10.1038/s41467-022-34871-9. PMID: 36435834; PMCID: PMC9701216.
83. Zhang J, Liu Y, Yu CJ, Dai F, Xiong J, Li HJ, Wu ZS, Ding R, Wang H. Role of ARPC2 in Human Gastric Cancer. *Mediators Inflamm.* 2017;2017:5432818. doi: 10.1155/2017/5432818. Epub 2017 Jun 13. PMID: 28694563; PMCID: PMC5485321.
84. Guan B, Wang TL, Shih IM. ARID1A, a factor that promotes formation of SWI/SNF-mediated chromatin remodeling, is a tumor suppressor in gynecologic cancers. *Cancer Res.* 2011 Nov 1;71(21):6718-27. doi: 10.1158/0008-5472.CAN-11-1562. Epub 2011 Sep 7. Erratum in: *Cancer Res.* 2012 Jun 15;72(12):3116. PMID: 21900401; PMCID: PMC3206175.
85. Mandal J, Mandal P, Wang TL, Shih IM. Treating ARID1A mutated cancers by harnessing synthetic lethality and DNA damage response. *J Biomed Sci.* 2022 Sep 19;29(1):71. doi: 10.1186/s12929-022-00856-5. PMID: 36123603; PMCID: PMC9484255.

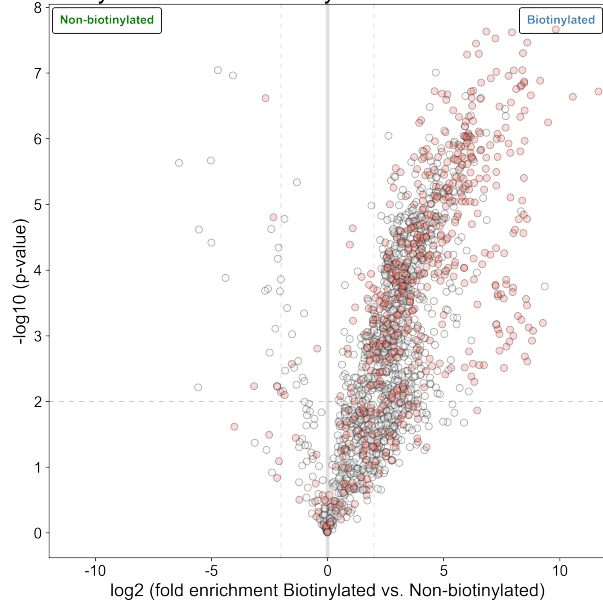
Supplementary

	Synthetic Lethal Target	Clinical Drug	Citation
Epigenetic Regulators	EZH2	Tazemetostat	Bilteer et al., 2015
	HDAC6	Ricolinostat	Bilteer et al., 2017
	HDAC2	Vorinostat	Fukumoto et al., 2018
	BRD2 (BET Family)	Molibresib	Bern et al., 2018
Kinase inhibitors	PLK-1	Volasertib	Srinivas et al., 2022
	PI3K	Copanlisib	Samartzis et al., 2014
	AKT	Capivasertib	Samartzis et al., 2014
	PARP	Olaparib	Shen et al., 2015
	Tyrosine Kinase	Dasatinib	Miller et al., 2016
	ATR	Ceralasertib	Williamson et al., 2016
	AURKA	Alisertib	Wu et al., 2018
Metabolic-related	Reactive Oxygen Species Induction	Elesclomol	Kwan et al., 2016
	GSH/GCLC	PRIMA-1Met	Ogiwara et al., 2019

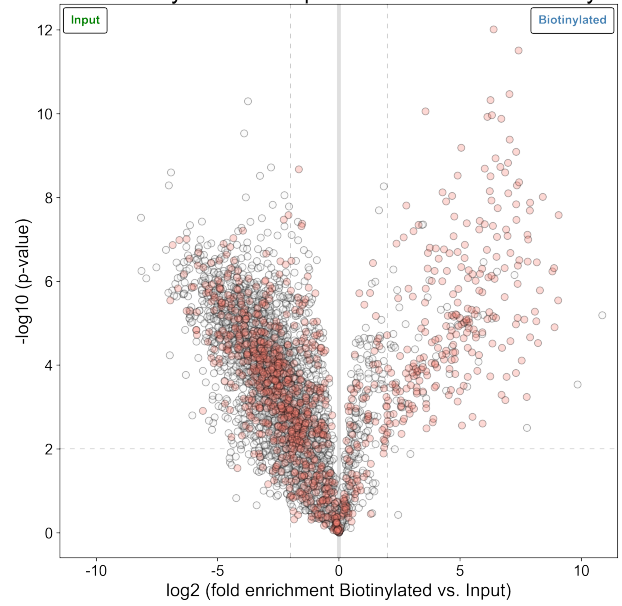
	Synthetic Lethal Target	Clinical Drug	Current testing phase
Epigenetic Regulators	EZH2	Tazemetostat	Human, Phase II (NCT05023655)
	HDAC6	Ricolinostat	Animal, Preclinical (Bitler et al., 2017)
	HDAC2	Vorinostat/SAHA (Pan-HDAC)	Animal, Preclinical (Fukumoto et al., 2018)
	BRD2 (BET Family)	Molibresib	Animal, Preclinical (Berns, et al., 2018)
Kinase inhibitors	PLK-1	Volasertib/Onvansertib	Animal, Preclinical (Srinivas, et al. 2022)
	PI3K	Copanlisib	Cell Line, Preclinical (Samartzis et al. 2014)
	AKT	Capivasertib	Cell Line, Preclinical (Samartzis et al. 2014)
	PARP	Olaparib	Human, Phase II with Ceralasertib (NCT04065269)
	Tyrosine Kinase	Dasatinib	Animal, Preclinical (Miller et al., 2016)
	ATR	Ceralasertib	Human, Phase II with Olaparib (NCT04065269)
	AURKA	Alisertib	Animal, Preclinical (Wu et al., 2018)
Metabolic-related	Reactive Oxygen Species Induction	Elesclomol	Cell Line, Preclinical (Kwan et al., 2016)
	GSH/GCLC	PRIMA-1Met	Patient-derived & Animal, Preclinical (Ogiwara et al., 2019)

Supplementary figure 1. Current synthetic lethal drugs available for ARID1A-mutant tumours and the corresponding clinical trials. Data and image courtesy – Norbert Tay

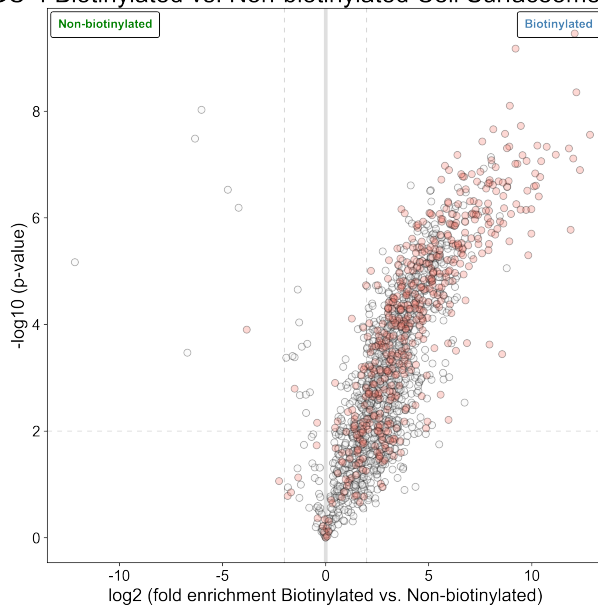
AGS Biotinylated vs. Non-biotinylated Cell Surfaceome Analysis



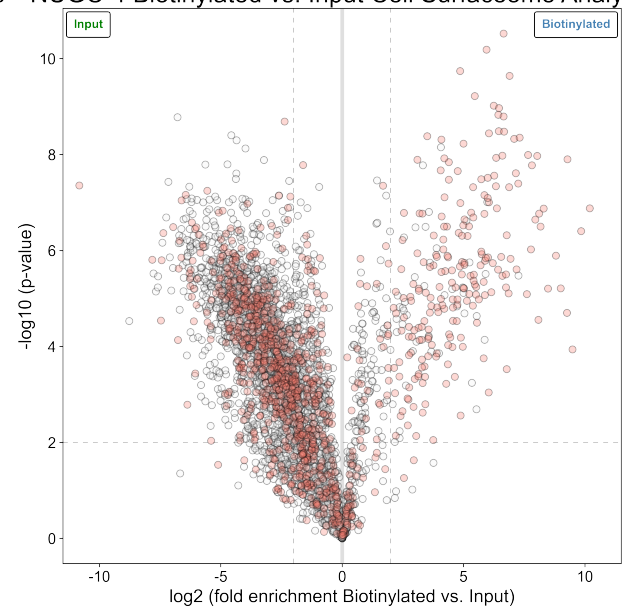
AGS Biotinylated vs. Input Cell Surfaceome Analysis



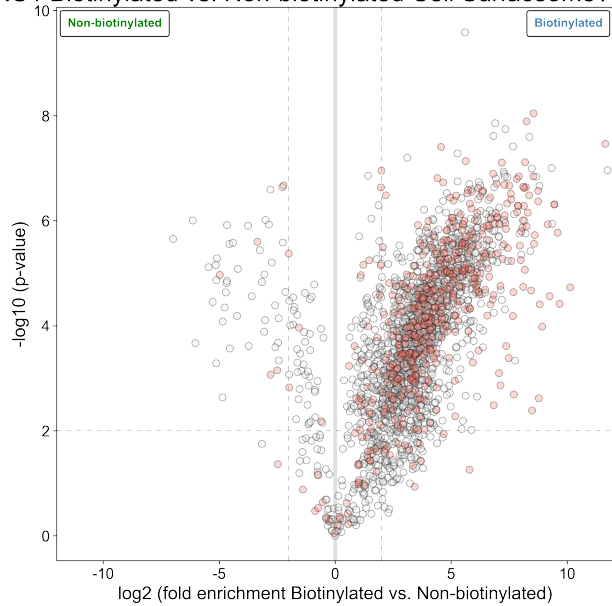
NUGC-4 Biotinylated vs. Non-biotinylated Cell Surfaceome Analysis



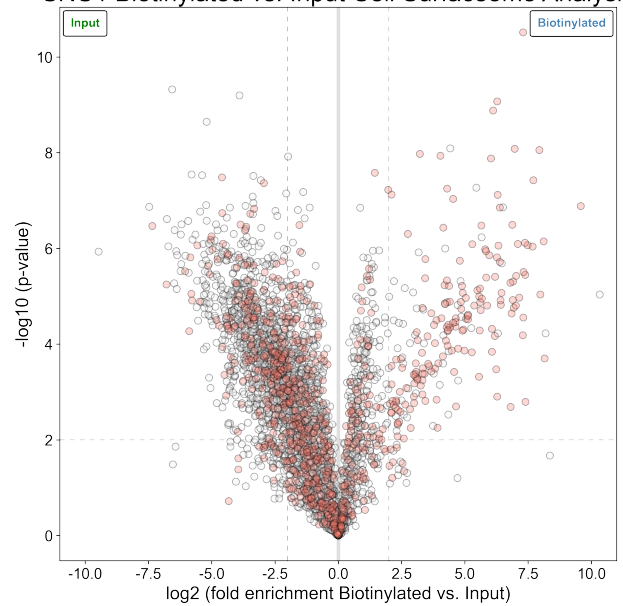
NUGC-4 Biotinylated vs. Input Cell Surfaceome Analysis



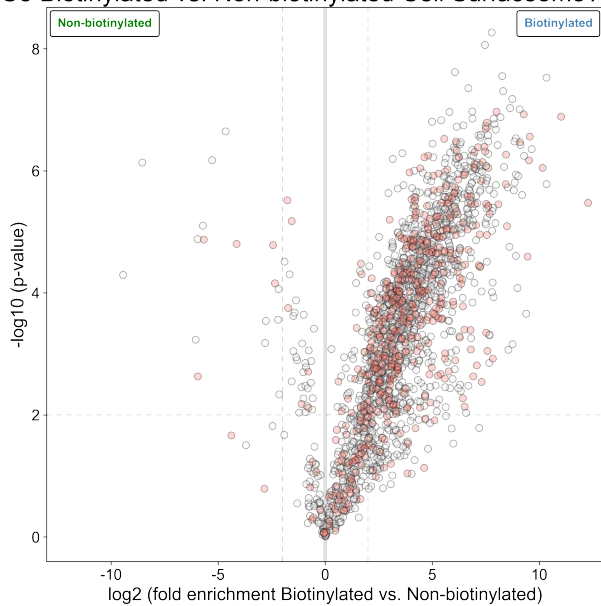
SNU1 Biotinylated vs. Non-biotinylated Cell Surfaceome Analysis



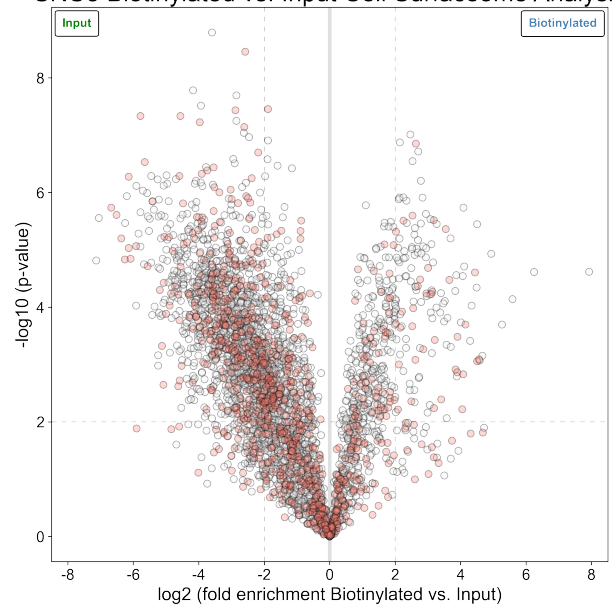
SNU1 Biotinylated vs. Input Cell Surfaceome Analysis



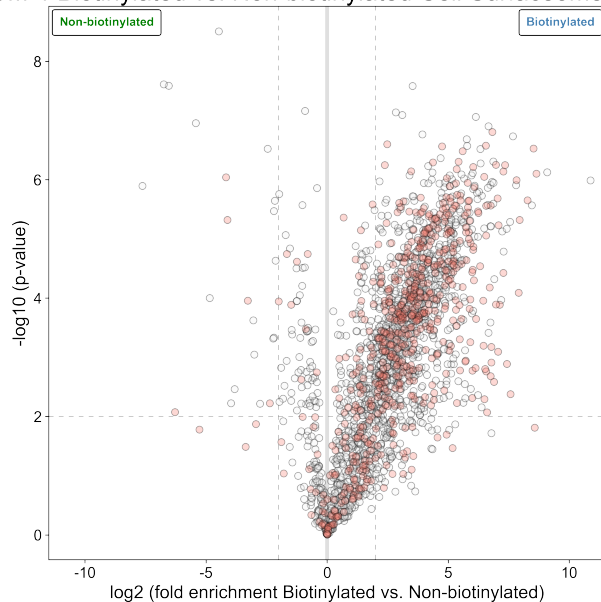
SNU5 Biotinylated vs. Non-biotinylated Cell Surfaceome Analysis



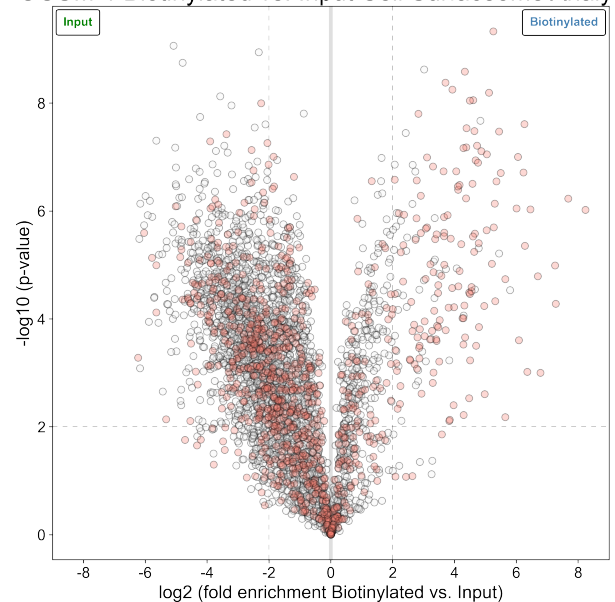
SNU5 Biotinylated vs. Input Cell Surfaceome Analysis



OCUM-1 Biotinylated vs. Non-biotinylated Cell Surfaceome Analysis



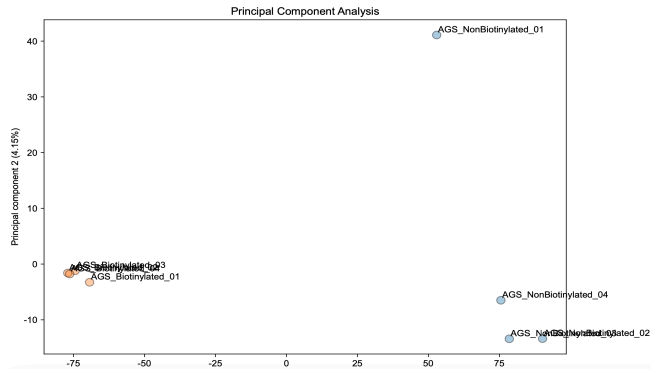
OCUM-1 Biotinylated vs. Input Cell Surfaceome Analysis



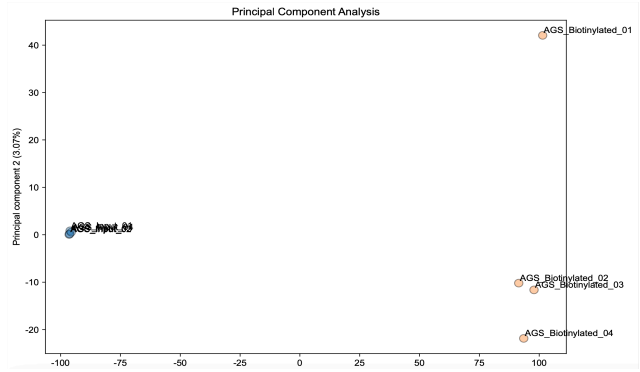
Supplementary Figure 2 a. Volcano plots showing enrichment of pull-down proteins in all the 5 cell lines – The plot shows the comparison between two controls 'Biotinylated vs Non-biotinylated' vs 'Biotinylated vs Input' for each of the cell lines. The orange dots represent the proteins that corresponds with the GO term 'Plasma Membrane'. For each cell line N=4 and significant proteins are determined by a value $> \log_2fc(2)$ and p-value < 0.01 .

AGS

Biotinylated vs Non-biotinylated

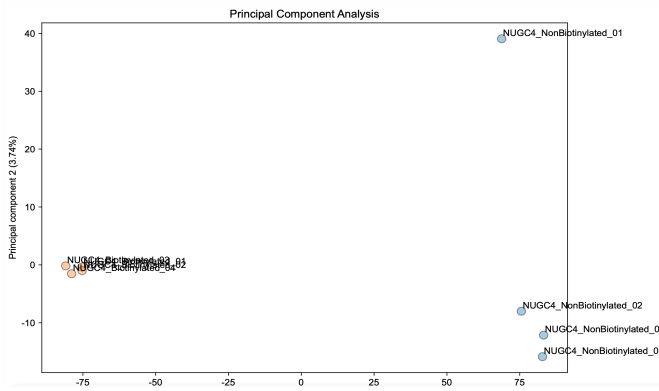


Biotinylated vs Input

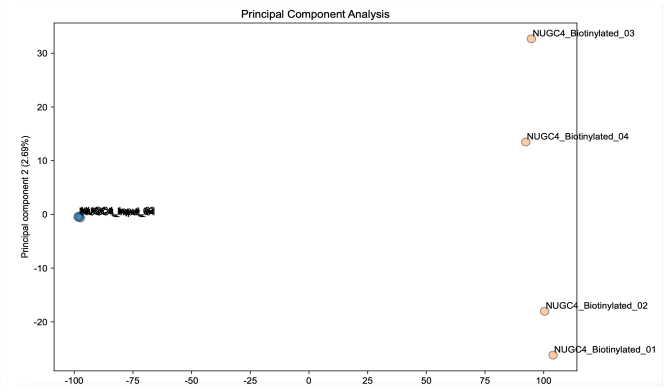


NUGC-4

Biotinylated vs Non-biotinylated

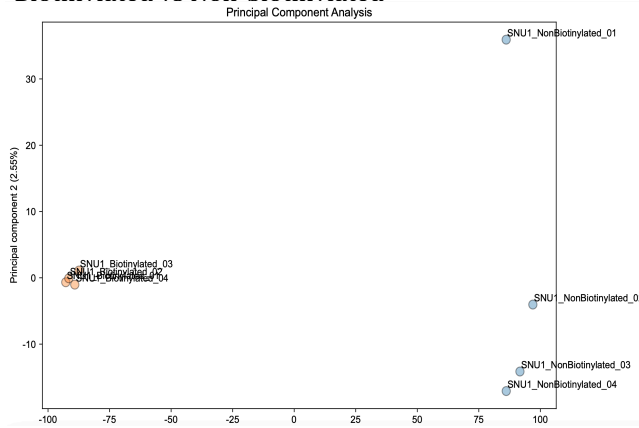


Biotinylated vs Input

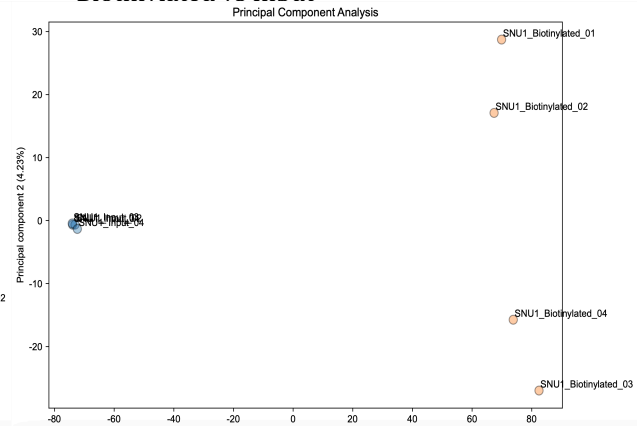


SNU-1

Biotinylated vs Non-biotinylated

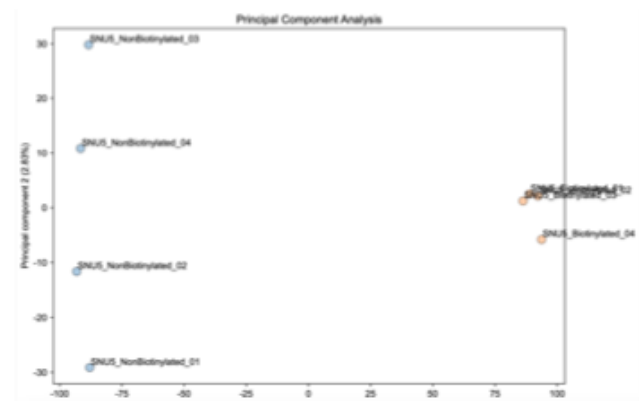


Biotinylated vs Input

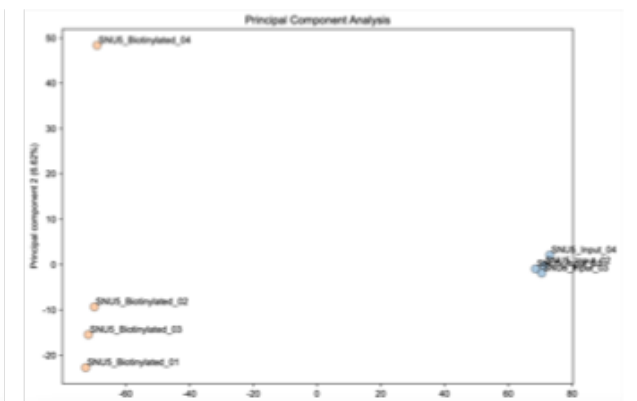


SNU-5

Biotinylated vs Non-biotinylated



Biotinylated vs Input

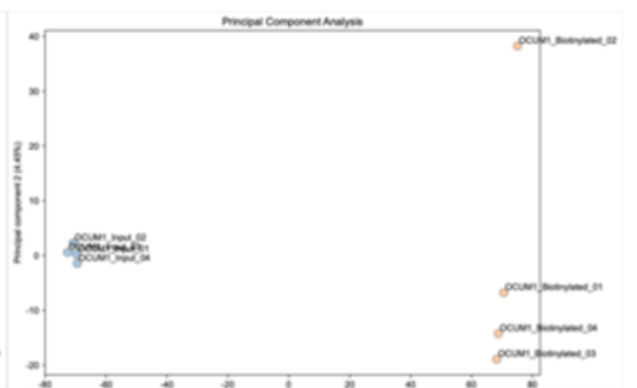


OCUM-1

Biotinylated vs Non-biotinylated



Biotinylated vs Input



Supplementary Figure 2 b. - PCA plots for enrichment of cell-surface proteins – The parameters for significantly enriched proteins remains the same as supplementary fig.2a. This is just a PCA plot of the same analysis.

Unique mutant surface proteins		Unique WT surface proteins				Common surface proteins mutant vs WT				
MIF	STOML2		CKAP4	ZDHHC5	CXADR	GPC1		EFNB1	HLA-C	RCC2
NDUFC2	ME2		BTN2A1	PCDH7	SYPL1	TNFRSF10A		SPTBN1	PVRL2	BSG
ATIC	MLEC		ESAM	IQGAP2	PVRL2	PRSS8		AP2B1	GNAI3	CNP
GPI	ATP6V1E1		SLC44A2	PRNP	PROCR	MSLN		ACLY	SLC3A2	DCXR
RAC1	SERPINB6		LTBR	CD81	GPC4	ADAM15		VAPB	ATP6V1A	ITGA6
DCBLD2	TSG101		ANO6	HSD17B10	CD55	CDCP1		EIF2B1	MPZL1	
GLG1	CDC42		PKP2	ITGA2	ATP1A1	CD46		SLC1A5	SLC7A5	
STOM	CSNK2A1		CEACAM1	FCGRT	SDC4	ITGB4		LNPEP	TNFRSF10B	
CAT	EFNB2		SRM	CTNNB1	PVRL3	FAM171A1		KHDRBS1	PGRMC1	
CAP1	VAMP3		SLC16A1	SLC39A10	ATP1B3	ADAM9		SCCPDH	ATP1A1	
EZR	CALM2		PPP5C	CNNM3	EGFR	SLC39A14		HLA-A	AP2A2	
KTN1	GNB2		CD99	ATP6V0D1	MMP14	ITGA5		FASN	NPTN	
SCARB2	GNA11		PLAUR	ERBB2	DSC2	RAB21		ITGAV	FAS	
MTDH	RIC8A		SIGIRR	LDLR	TSPAN8	ST14		GNA13	AP2A1	
FH	VDAC1		SLC12A2	RAB18	NCSTN	ITM2B		RELL1	M6PR	
PTPN1	LMAN2		ERBB3	KITLG	CLDN4	PPP3CA		RTN4	ATP1B3	
CSNK2B	ANXA1		PVRL1	EPCAM	TFRC			ITGB1	VAPA	
BCAP31	KARS		SMPDL3B	TLN1	SPINT1			GRB2	LAMP1	
CALR	ASPH		SLC39A6	EPHA1	HLA-B			APP	EPHA2	
GNAI2	P4HB		MMP15	CD47	FLRT3			ATP6AP1	DSG2	
TPBG	CPNE3		PKP4	PLXNB1	TSPAN15			FMR1	ESYT1	
MAPK1	TWF1		CD97	PTPRF	ALCAM			PTPRK	CD46	
CRKL	SEPT7		ITGB5	EPS8L2	ERBB2IP			PPP2R1A	PARK7	
SDHB	HSPD1		FLOT2	BCAM	CD276			CHP1	TFRC	
GNB1	LANCL2		TYRO3	IFNGR1	ITGAV			DAG1	PVR	
PCYOX1	APLP2		PVRL4	ICOSLG	CD44			SDCBP	SDC1	
CLIC1	RAB7A		RAP2B	COMT	MET			ATP5O	HSPA5	
DPYSL2	TKT		SLC44A1	TMPRSS4	PTPRK			SYPL1	PON2	
PDIA6	PI4K2A		NOTCH1	PCDH1	SEMA4B			MYH9	ATP1B1	
GLO1	MFGE8		CNNM4	LSR	CHP1			GSR	NCSTN	
ATP6V1B2	SEPT2		ITGA3	PTPRA	MUC1			ATP6V1C1	ADAM9	
DDOST	C1QBP		CD59	MST1R	OCLN			EPHB4	PLXNB2	
NCEH1	NCL		TESC	BTN3A3	INSR			ADAM10	ABHD12	
GOT2	ARPC2		RTN4R	PLXNA1	SLC3A2			SCARB1	RAB5C	

Supplementary Figure. 3 - List of genes from MS analysis - The list includes significantly enriched ($\log_2fc(2)$ and p -value <0.01) unique and common cell-surface proteins in the ARID1A mutant cell lines and the ARID1A-WT cell lines. 68 unique proteins in the mutant group, 146 unique proteins in WT group and 73 common proteins.

